Colloquium: Neutrino detectors as tools for nuclear security

Adam Bernstein[*] and Nathaniel Bowden[†]

Nuclear and Chemical Sciences Division, Lawrence Livermore National Laboratory, Livermore, California 94550, USA

Bethany L. Goldblum[‡]

Department of Nuclear Engineering, University of California, Berkeley, California 94720, USA

Patrick Huber[§]

Center for Neutrino Physics, Virginia Tech, Blacksburg, Virginia 24061, USA

Igor Jovanovic[‖]

Department of Nuclear Engineering and Radiological Sciences, University of Michigan, Ann Arbor, Michigan 48109, USA

John Mattingly[¶]

Department of Nuclear Engineering, North Carolina State University, Raleigh, North Carolina 27695, USA

(published 12 March 2020)

For over 40 years, physicists have considered possible uses for neutrino detectors in nuclear nonproliferation, arms control, and fissile materials security. Neutrinos are an attractive fission signature because they readily pass through matter. The same property makes neutrinos challenging to detect in systems that would be practical for nuclear security applications. This Colloquium presents a broad overview of several potential neutrino applications, including the near-field monitoring of known reactors, far-field monitoring of known or discovery of undeclared reactors, detection of reactor waste streams, and detection of nuclear explosions. Recent detector advances have made near-field monitoring feasible, whereas farther-field reactor detection and waste stream detection monitoring may be possible in some cases with further research and development. Very long-range reactor monitoring and nuclear explosion detection do not appear feasible for the foreseeable future due to considerable physical and/or practical constraints.

DOI: 10.1103/RevModPhys.92.011003

CONTENTS

[*]bernstein3@llnl.gov
[†]nbowden@llnl.gov
[‡]bethany@nuc.berkeley.edu
[§]pahuber@vt.edu
[‖]ijov@umich.edu
[¶]jkmattin@ncsu.edu

I. INTRODUCTION

The advent of nuclear weapons as the first practical application of nuclear fission profoundly affected the dynamics of international relations. The destructive potential of nuclear weapons rendered conflicts in which they could be used potentially catastrophic, with weapons effects far surpassing those of conventional armaments. The effects of nuclear weapons cannot be constrained to the location where they are used, because of the subsequent radioactive fallout and potential multiyear effects on the global climate. While the United States and the USSR avoided using nuclear weapons throughout the Cold War, both took part in an arms race that, at its apex in 1986, resulted in a stockpile of an estimated 63 000 warheads (Kristensen and Norris, 2013). During the Cold War and afterward, nuclear weapons proliferated, the production of special nuclear materials continued, and nuclear knowledge spread across the globe, even in states that did not have nuclear weapons, creating another major risk, nuclear terrorism. Today we are faced with nine countries having a total of nearly 15 000 nuclear weapons and there are additional countries at the verge of or actively seeking a nuclear weapons capability (Kristensen and Norris, 2017).

Recognition of these unique challenges led to major international efforts to curb the testing and use of nuclear technology for the purpose of nuclear warfare and to bolster nuclear security. To gain more coherence and legitimacy, these efforts have been articulated through several international treaties, most notably the Treaty on the Non-proliferation of Nuclear Weapons (NPT), which came into force in 1970. While the NPT provides an institutional and legal framework to curb proliferation, it also requires the development and adoption of effective technical measures for verification.

Applied antineutrino physics has the potential to provide novel verification technologies, especially with regard to plutonium production and diversion. First we give a brief summary of the current safeguards framework. Next we provide an overview of the current state of knowledge and opportunities for future technical developments in the area of antineutrino detection for nuclear security with a focus on four areas: monitoring of fissile material production, discovery and exclusion of undeclared reactors, monitoring of spent fuel and reprocessing waste, and confirmation of nuclear explosions. For each of these applications we discuss the current technical means of verification and highlight additional capabilities offered by antineutrino detection.

II. CURRENT SAFEGUARDS FRAMEWORK

The Treaty on the Non-Proliferation of Nuclear Weapons (United Nations Office for Disarmament Affairs, 1968) is the central pillar of the international legal framework addressing the security challenges arising from nuclear weapons. It has been in force since 1970 and has 191 signatories, making it the most widely accepted arms control and disarmament agreement to date.

The control of fissile materials[1] is the central concern in nuclear security as already recognized in 1946 (Lilienthal *et al.*, 1946). Under the NPT, non-nuclear-weapon[2] state parties to the Treaty are required to declare their "source of special fissionable material in all peaceful nuclear activities," which includes civilian nuclear power production. To ensure proper accounting of this nuclear material of proliferation concern, states conclude comprehensive safeguard agreements or voluntary offer agreements with the International Atomic Energy Agency (IAEA), where fissile material production is monitored via inspections and accounting measures. All stages of the nuclear fuel cycle are subject to IAEA safeguards; this includes uranium mining, uranium enrichment, fuel fabrication, use in a reactor, spent nuclear fuel (SNF), and, where applicable, reprocessing. There are currently 454 operating civilian nuclear power reactors in the world with dozens more under construction (World Nuclear Association, 2019), and thus monitoring of fissile material production at known nuclear reactor facilities is a key challenge for the IAEA.

An additional challenge in verifying the NPT is confirming that a nation has declared all of its nuclear material and activities. Such a task is hindered by the need to continuously verify the absence of undeclared nuclear reactors, materials, and weapons-relevant activities. The detection of undeclared nuclear reactors has historically been largely supported through national technical means, which involves the collection and analysis of materials, reactor emanations, and other information by individual states to verify compliance with international agreements (Stubbs and Drell, 2013).

Nuclear-related turmoil occurring at the end of the Cold War, including the covert Iraqi nuclear weapons program (Davis and Kay, 1992), the refusal of North Korea to allow certain IAEA inspections (Hecker, Carlin, and Serbin, 2018), and uncertainty surrounding the status of South Africa's nuclear program (Stumpf, 1996), led the IAEA and the international community to recognize that existing safeguard measures failed to provide a complete picture of a state's nuclear activities. In response, the Model Additional Protocol (IAEA, 1998) was created to supplement existing cooperative IAEA safeguards with strengthened measures, designed to provide greater assurance for detection of undeclared nuclear materials and activities. The measures include the incorporation of satellite imagery and other open-source data, and access to information was also increased through an expanded scope of reporting, declarations, and complementary access to nuclear sites. The Model Additional Protocol also emphasized a balancing need for nonintrusive monitoring approaches. While the Model Additional Protocol has already significantly bolstered IAEA safeguards, limitations remain—both procedural and technical—that leave open the possibility that undeclared nuclear reactors go undetected (Findlay, 2007).

[1]Fissile materials are defined by their ability to sustain a nuclear chain reaction with neutrons of thermal energy, e.g., ^{235}U and ^{239}Pu.

[2]Non-nuclear-weapon states are defined as state parties to the NPT that did not manufacture and explode a nuclear weapon or other nuclear explosive device before 1 January 1967.

The production of nuclear energy results in the generation of radioactive waste, including SNF that has been removed from the reactor core and any waste materials that remain after the SNF has been processed. Fission product decays are present in SNF and reprocessed waste, although at a declining rate depending upon the amount and age of the material in a storage facility or repository. The IAEA implements technical verification measures for the back end of the nuclear fuel cycle, including SNF storage, reprocessing, and long-term disposition (Pushkarjov and Tkharev, 1986). NPT signatory states are obligated to declare the uranium and plutonium content of SNF and, currently, thousands of significant quantities (SQs)[3] of plutonium in SNF are under IAEA safeguards. The majority of SNF is from light water reactors, but the fuel from heavy water-moderated and gas-cooled graphite-moderated reactors also contains plutonium, which may be particularly well suited for nuclear weapons fabrication. The IAEA currently employs containment and surveillance to confirm the presence of the fuel assemblies using seals on the reactor vessel while the fuel is still in use and seals on dry storage casks when the SNF is sent to permanent storage. While these approaches may be satisfactory in some scenarios, they require that the integrity of the items is preserved—the so-called continuity of knowledge needs to be maintained.

New international agreements may also shape the safeguards landscape, such as a proposed Fissile Material Cutoff Treaty (FMCT) (Nuclear Threat Initiative, 2018). In its most limited version, an FMCT would ban the production of additional fissile materials—in practice, highly enriched uranium and separated plutonium—for nuclear weapons. A significant number of countries would support an expanded treaty that would include the reduction of existing stocks of fissile materials available for nuclear weapons by placing agreed-upon quantities of nonsafeguarded fissile materials not currently in nuclear weapons under international safeguards. While an FMCT has thus far failed to find political traction, progress toward such an agreement would enhance the need for robust technical means for SNF monitoring and discovery.

Finally, the Comprehensive Test Ban Treaty (CTBT) bans nuclear explosions on any scale (United Nations Office for Disarmament Affairs, 1996). The CTBT was opened for signature in 1996 and will come into force when 44 specified states that possessed nuclear reactors as of certain dates in the 1990s have ratified it. Currently, eight of these states—China, the Democratic People's Republic of Korea, Egypt, India, Iran, Israel, Pakistan, and the United States—have yet to ratify the treaty. Nonetheless, the CTBT has created a near-universal global norm against nuclear explosion testing and international efforts are maintained related to the nuclear explosion monitoring mission.

III. PHYSICS OF NEUTRINOS FROM FISSION SOURCES

Nuclear reactors, nuclear explosions, and reactor waste streams produce neutrinos by the same primary mechanism: nuclear beta decay. Detection approaches are likewise related, although detection feasibility varies depending on the source type and distance from source to detector.

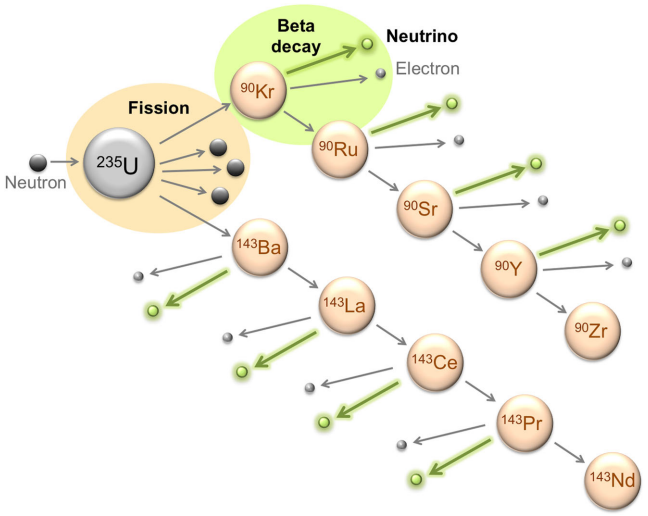

FIG. 1. An example of beta decay chain of fission fragments resulting in the emission of eight neutrinos. Figure courtesy of R. Carr.

A. Neutrino production in fission sources

Neutrinos are produced not by fission itself but the beta decay of fission fragments.[4] Typically, one fission produces two fragments. Each of these neutron-rich fragments decays an average of 3 times. Each decay produces one electron antineutrino[5]:

$$ {}^{A}_{Z}N \rightarrow {}^{A}_{Z+1}N' + e^{-} + \bar{\nu}_{e}. \tag{1}$$

Thus, one fission leads to the emission of roughly six neutrinos. Figure 1 illustrates this process.

Details of the neutrino flux vary according to the nature of the fission source. Most importantly, the neutrino flux depends on which nuclides undergo fission, while the energy of the fission-inducing neutrons has a smaller impact (Littlejohn *et al.*, 2018). The dominant nuclides in most reactors and explosions are ^{235}U, ^{239}Pu, ^{238}U, and ^{241}Pu. Neutrino emissions from these nuclides differ because the fission fragment yields differ. The left side of Fig. 2 shows the fission fragment yields. As these distinct populations of fission fragments decay toward stability, they give rise to different emission rates and spectra of neutrinos. The right side of Fig. 2 illustrates how the neutrino flux measured via inverse beta decay, a common detection mechanism described in Sec. III.B, varies between nuclides. Notably, ^{235}U produces about 50% more detectable neutrinos per fission than ^{239}Pu, with a harder energy spectrum. The neutrino flux from a single source often

[3]The IAEA defines 1 significant quantity (1 SQ) of plutonium as 8 kg of total plutonium provided the ^{238}Pu content is less than 80%.

[4]Beta decays following neutron capture on materials in a reactor also contribute to the neutrino flux. The effect is small for typical power reactors (Huber and Jaffke, 2016), but can be significant for certain research reactor configurations (Ashenfelter *et al.*, 2019).

[5]Following common usage, this review uses "neutrino" as a general term for both neutrinos and antineutrinos.

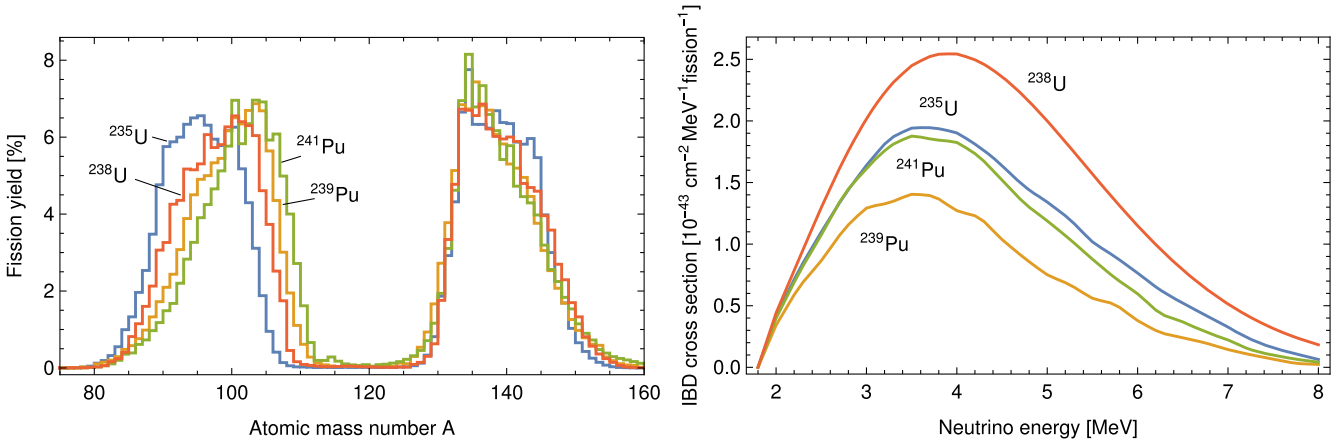

FIG. 2. Left: Fission fragment yields from the four major nuclides in fission sources according to JEFF 3.3 (Nuclear Energy Agency, 2017). Right: The detection cross section per fission for neutrinos from each of the four fissile isotopes, which is obtained as the product of IBD cross section and the neutrino flux.

includes contributions from fission of multiple nuclides. For example, in a reactor fueled with low-enriched uranium (LEU), some neutrinos come from fissions of ^{235}U and some from fissions of ^{239}Pu bred in by neutron capture on ^{238}U. The overall neutrino flux is a function of the total fission rate $R(t)$, the fraction of fissions occurring on the kth nuclide $\alpha_k(t)$, and the neutrino flux from the kth fissioning nuclide $S_k(E_\nu, t)$, where E_ν is neutrino energy and t is time.

Neutrino emissions from a single source often change over time. In a reactor, the timescale for significant changes in R and α_k (hours to days) is much longer than most of the beta decay lifetimes (mostly less than a minute). This means that the neutrino flux from a reactor can be given by the equilibrium expression

$$\phi_\nu^{\text{equil}}(E_\nu, t) = R(t)\sum_k \alpha_k(t) S_k(E_\nu, t). \tag{2}$$

Equation (2) can also be rewritten in terms of the reactor thermal power $P_{\text{th}} = R\sum_k \alpha_k E_k$, where E_k is the mean energy per fission of the kth nuclide:

$$\phi_\nu^{\text{equil}}(E_\nu, t) = \frac{P_{\text{th}}(t)}{\sum_k \alpha_k(t) E_k} \sum_k \alpha_k(t) S_k(E_\nu, t). \tag{3}$$

By contrast, in a nuclear explosion, all fissions occur nearly instantaneously. The burstlike neutrino emission from an explosion cannot be approximated by an equilibrium expression. Nonetheless, the general logic of Eq. (2) holds: the neutrino flux from an explosion is a product of the total number of fissions (proportional to the fission yield of the explosion) and the sum of neutrino fluxes from each fission fragment nuclide, weighted by the fraction of fissions occurring on each nuclide.

Even in a reactor, some notable effects are not covered by the equilibrium approximation of Eqs. (2) and (3). One such effect is the emission of neutrinos from nuclear fuel after the reactor is shut down or after the fuel is removed. This emission comes from the small fraction of fission fragments that beta decay over long timescales. These are the same decays responsible for the long-term gamma and beta radioactivity of used nuclear fuel. The neutrino rate from irradiated fuel, whether stored in casks or modified through chemical reprocessing, is much lower than that from operating reactors, and the energy spectrum from used fuel is also softer.

Table I compares the production of neutrinos in the three sources we consider in this Colloquium: reactors, explosions, and waste streams from reactors. Recall that the basic production mechanism is the same for all sources, namely, the beta decay of fission fragments. The energy dependence, time dependence, and relative intensity of the neutrino flux vary among these three sources, with implications for the practicality of applications. All of these sources emit neutrinos isotropically. The fusion reactions most common in nuclear

TABLE I. Comparison of the three sources of neutrinos discussed in this Colloquium.

Source	Main origin of $\bar{\nu}_e$	Time profile of $\bar{\nu}_e$ emission	Energy of $\bar{\nu}_e$ emitted	History of $\bar{\nu}_e$ from this source
Nuclear reactor	Beta decay of fission fragments	Moderate, quasisteady state emission over days to months	Up to ~8 MeV	First detected 1956; millions of interactions detected in many subsequent experiments
Nuclear explosion	Beta decay of fission fragments	Intense burst over a few seconds	Up to ~8 MeV, with higher energies emitted earlier	No known detections of $\bar{\nu}_e$ from this source
SNF and fuel reprocessing waste	Beta decay of fission fragments with long lifetimes	Low-level emission that exponentially decays over many years	Up to ~3 MeV	Likely detected in reactor $\bar{\nu}_e$ experiments but so far indistinguishable from reactor signal and other backgrounds

weapons and the reactions under consideration for fusion power plants do not produce neutrinos.

B. Basics of detecting fission neutrinos

Equations (2) and (3) hint at the information carried by neutrino emissions from fission sources. To capture this information, one must observe the neutrinos interacting in a detector. Consider the generic case of detecting neutrinos some distance L from a fission source with neutrino flux ϕ_ν. Where the spatial extent of the source is small compared to L, the number of detectable neutrino events $N_{\rm det}$ is

$$N_{\rm det}(E_\nu, t) = \frac{\epsilon(E_\nu)}{4\pi L^2}\phi_\nu(E_\nu, t)\sigma(E_\nu)N_T P_{\rm surv}(E_\nu, L). \quad (4)$$

In this expression, ϵ is the signal detection efficiency, σ is the cross section for the interaction to which the detector is sensitive, N_T is the number of interaction targets in the detector, and $P_{\rm surv}$ is the electron antineutrino survival probability.

Soon after the neutrino was postulated, it was recognized that neutrino cross sections will be very small and that the most likely reaction is inverse beta decay (IBD) (Bethe and Peierls, 1934) with a cross section of $\approx 10^{-43}$ cm^2. The target of this reaction is a free proton (hydrogen nucleus):

$$\bar{\nu}_e + p \rightarrow e^+ + n. \quad (5)$$

The threshold for this reaction is $m_n - m_p + 2m_e \simeq 1.8$ MeV and the visible energy of the positron is given by $E_{\rm vis} = E_\nu - 1.8\ {\rm MeV} + 2 \times 0.511\ {\rm MeV}$, that is, there is a one-to-one correspondence between detected energy and the neutrino energy E_ν (Vogel and Beacom, 1999). The correspondence arises from kinematics: the energy of the neutrino is carried by the positron and the momentum by the neutron, where the kinetic energy of the neutron is indeed very small, on average about 50 keV. As a consequence, energy reconstruction for the neutrino is straightforward but measuring its direction is difficult. The positron will deposit its energy promptly and the neutron will thermalize and then capture on either hydrogen or a specifically added neutron-capture target like gadolinium or lithium; the neutron-capture elements have a high thermal neutron-capture cross section. This allows one to exploit a delayed coincidence between the prompt positron signal and the delayed neutron-capture signal: both events happen close in time 10–200 μs and space 5–15 cm. The neutron-capture signature can be emission of either gamma rays, in the case of cadmium or gadolinium, or alpha particles and tritons in the case of lithium. These signatures together form the basis for detector design since the discovery of neutrinos (Cowan *et al.*, 1956) and greatly suppress backgrounds from natural radioactivity and cosmic rays. Inverse beta decay on other nuclei besides hydrogen is possible, but generally the cross section is suppressed by nuclear matrix elements and there are fewer targets per unit mass, making hydrogen by far the most practical choice. Suitable detector mediums contain hydrogen and are transparent: organic scintillators and water. They both convert the ionization signals of the positron and neutron capture into light by either scintillation or Cerenkov radiation.

Interaction modes other than IBD exist: typically they are less practical, but they can offer certain advantages. In the case of neutrino-electron scattering

$$\bar{\nu} + e^- \rightarrow \bar{\nu} + e^-, \quad (6)$$

the advantage is that the scattered electron direction may be easier to reconstruct than the initial momenta of IBD products. This may be useful for localizing a fission source such as an undeclared reactor. Backgrounds are often a challenge for this single reaction product (Hellfeld *et al.*, 2017). In the case of coherent elastic neutrino-nucleus scattering (CEνNS)

$$\bar{\nu} + N \rightarrow \bar{\nu} + N, \quad (7)$$

one advantage is that the cross section is coherently enhanced by the contribution of all neutrons in the target nucleus (Freedman, 1974). For a large nucleus such as germanium or xenon, the enhancement is 2 orders of magnitude over IBD per unit detector mass. Another advantage is that CEνNS has no kinematic threshold, so neutrinos below the IBD threshold of 1.8 MeV are in principle observable. For CEνNS, the primary difficulties are detecting the very low-energy nuclear recoil, typically $\mathcal{O}(10\text{–}100)$ eV, and suppressing background in this low-energy range. Owing to these small recoil energies, this reaction has been observed only recently (Akimov *et al.*, 2017), albeit using neutrinos from a pulsed source with about 10 times higher average energy than reactor neutrinos.

The final component of Eq. (4) accounts for neutrino flavor oscillation. This is the quantum mechanical phenomenon that allows a neutrino created in one flavor (electron, muon, or tau) to be detected as a different flavor (Kajita, 2016; McDonald, 2016). Fission sources produce only electron antineutrinos, and IBD is sensitive only to this flavor. When electron antineutrinos propagate, some of them become invisible to IBD detectors as they oscillate into nonelectron flavors; only the surviving electron antineutrinos are observable. One upside of oscillations is that $P_{\rm surv}$ has a nonlinear dependence on L, the distance from source to detector. Thus oscillations can break certain degeneracies (Jocher *et al.*, 2013). The more essential upside is that neutrino oscillations are a major focus of basic research. The presence of oscillations in Eq. (4) has made reactors a key source for fundamental physics experiments. These experiments have played a critical role in developing technology that may be used for neutrino applications.

Neutrinos interact only via the weak force, and thus, neutrino cross sections are very small in absolute terms. Consequently, neutrino detection requires careful control and reduction of potential background sources. Common strategies are the selection of radio-clean construction materials, the use of engineered shielding against neutrons and gamma rays, locating the experiment underground, particle identification, and spatial segmentation. For a more detailed discussion, which is beyond our scope, see, for instance, Bowden, Sweany, and Dazeley (2012).

C. Information content of fission neutrino signals

The information contained in fission neutrino signals is described by Eqs. (2)–(4). Substituting Eq. (3) into Eq. (4) and suppressing the energy and time dependence for simplicity yields

$$N_{\mathrm{det}} = \left(\frac{\epsilon N_T \sigma}{4\pi}\right)\left(\frac{P_{e\to X}(L)}{L^2}\right)\frac{P_{\mathrm{th}}}{\sum_k \alpha_k E_k}\sum_k \alpha_k S_k. \quad (8)$$

The first factor in parentheses contains parameters which the detector operator can determine. The last parameter S_k is also fairly well known for the major nuclides, when fissioned by thermal neutrons.

In this context it is necessary to point out that reactor antineutrino fluxes have been the subject of intense scrutiny since 2011, when two new evaluations were conducted (Huber, 2011; Mueller *et al.*, 2011) that upcorrected the resulting IBD rates by approximately 6%. This in turn gave rise to the so-called reactor antineutrino anomaly (RAA) (Mention *et al.*, 2011): all past measurements, which had been interpreted as being in agreement with prior flux predictions, now indicated a significant rate deficit relative to those more modern updates. One possible solution could be the existence of a fourth, so-called sterile neutrino, which triggered considerable experimental activity (Abazajian *et al.*, 2012) and to date remains a viable possibility (Dentler *et al.*, 2018). The RAA and other discrepancies in prediction and measurements of the neutrino spectrum are under active study [for a review, see Hayes and Vogel (2016)], and it is clear that for applications these issues need to be resolved by experimental measurement. Therefore, calibrating reactor antineutrino fluxes from a range of different reactors at different stages in their fuel cycle is a mandatory, and entirely feasible, ingredient for this application. As an example consider the recent measurement of the neutrino yield spectrum from uranium-235 and plutonium-239 by the Daya Bay Collaboration (Adey *et al.*, 2019).

The other factors depend on information which the detector operator may not know: the distance L to the reactor (unknown if, for example, the reactor is hidden), the reactor power level P_{th}, and the fission fractions α_k inside the reactor core. Evidently, by observing neutrino emissions from the reactor, one can possibly infer a combination of the following:

- how far away the reactor is,
- what power level the reactor is operating at, and
- what the reactor is burning for fuel.

These pieces of information can be in principle distinguished using the time and energy dependence of the observed neutrino flux. Furthermore, one or more of these source characteristics may be constrained by non-neutrino data or by declared reactor operating histories. In this case, a combined analysis of neutrino and non-neutrino data could further disentangle these components. The assumption is that for deployments under cooperative safeguards the distance to the reactor is known at the percent level.

In a similar manner, the neutrino signal from a nuclear explosion carries information about how far away the explosion occurred, how much fission yield the explosion contained, and which nuclide was used as a nuclear explosive. Neutrino emissions from SNF carry some information about the fuel location and time elapsed since the fuel has been discharged from the reactor. However, as described in Secs. V–VIII, collecting this information is more practical near reactors than from waste streams or explosions. To give context for those comparisons, Sec. IV describes the history of neutrino detection at fission sources.

IV. HISTORY OF FISSION NEUTRINO DETECTION

A. Fundamental physics: First detection and neutrino oscillation experiments

The first detection of a neutrino of any kind occurred at a nuclear reactor. In the 1950s, a team led by Frederick Reines and Clyde Cowan observed neutrino emission from a plutonium production reactor at the U.S. Atomic Energy Agency (now Department of Energy) Savannah River site (Cowan *et al.*, 1956). The Cowan-Reines detector was small (<0.5 ton), but its use of an organic scintillator, doping, and segmentation established design principles that remain in use 60 years later. Over 5×10^6 neutrinos have now been detected at nuclear reactors around the world. Physicists, including Reines, considered making basic physics measurements using nuclear weapon tests as a source (Reines, 1995). To date, however, no neutrinos from nuclear explosions have been observed. Neutrinos from SNF make some contribution to data sets collected at nuclear power plants, but that component is not statistically distinguishable from the much larger contribution from operating reactors. Reactors remain the only fission source from which neutrinos have been conclusively detected.

As the brightest neutrino sources on Earth, nuclear reactors have attracted particle physicists over many decades for dozens of fundamental studies. Early experiments used ton-scale detectors located within a few tens of meters of reactor cores. Efforts searching for evidence of neutrino oscillation were mounted in the 1970s through the 1990s in the USA (Reines, Sobel, and Pasierb, 1980; Greenwood *et al.*, 1996; Riley *et al.*, 1999), France (Kwon *et al.*, 1981; Cavaignac *et al.*, 1984; Declais *et al.*, 1995), Switzerland (Zacek *et al.*, 1986), and the USSR (Kuvshinnikov *et al.*, 1991; Vidyakin *et al.*, 1994). In the late 1990s, the Chooz (Apollonio *et al.*, 1999) and Palo Verde (Boehm *et al.*, 2001) experiments extended the baseline for reactor neutrino oscillation searches to ≈1 km using detectors of 10 ton scale. In the early 2000s, the KamLAND experiment in Japan used a kiloton-scale liquid scintillator (LS) detector to observe neutrinos from nuclear reactors over 100 km away (Eguchi *et al.*, 2003). The energy-dependent deficit of electron antineutrinos seen by KamLAND, a consequence of flavor oscillations, helped to establish the fact that neutrinos have mass. More recently, LS detectors on the 10 ton scale have made precision oscillation measurements at distances in the range of 400–1900 m from nuclear power plants in China (An *et al.*, 2012), Korea (Ahn *et al.*, 2012), and France (Abe *et al.*, 2012). Beyond measuring fundamental neutrino parameters, these recent experiments provided stringent tests of the reactor neutrino emission models by performing high precision energy spectrum measurements.

The fundamental physics experiments previously described laid the foundation for possible reactor monitoring applications using neutrino emissions. They provide detection capability demonstrations at stand-off distances spanning the near field and far field, while also developing an understanding of reactors as a neutrino source and the important background mechanisms that limit sensitivity.

B. Application-oriented experiments

The fact that reactor neutrinos could be useful for nuclear security was recognized in 1978 by Mikaelyan and Borovoi (Borovoi and Mikaelyan, 1978; Mikaelyan, 1978). Several demonstrations of the reactor monitoring concept have been performed in the very near-field range, 7–25 m from reactors. Pioneering work was undertaken in the 1980s at the Rovno power plant in the former Soviet Union (Klimov *et al.*, 1994). This demonstration used a 0.5-ton, Gd-doped LS (GdLS) detector deployed in a below-ground gallery about 20 m from the reactor core. This high-efficiency detector recorded almost 1000 neutrino interactions per day with a signal-to-background (S:B) ratio considerably greater than unity. Over several years, this group demonstrated rapid determination of reactor on or off state transitions, tracking of reactor power levels, and measurements of the change in neutrino rate and spectrum due to fuel evolution (burnup); see Fig. 3.

The next effort to focus on reactor monitoring was based at the San Onofre Nuclear Generating Station (SONGS) in the United States. Beginning in the early 2000s, physicists from the Lawrence Livermore and Sandia National Laboratories constructed and deployed several neutrino detectors. The goal was to demonstrate that simple designs could operate unattended for long periods, collecting neutrino data suitable for reactor monitoring. The 0.6-ton, GdLS SONGS1 detector was deployed in a below-ground gallery about 20 m from the reactor (Bowden *et al.*, 2007). The device was calibrated automatically and maintained stable operation from 2003 until 2008. The simple design yielded a modest efficiency, with about 500 IBD events recorded per day. Analysis of the SONGS1 data set produced monitoring demonstrations similar to those achieved at Rovno: reactor state (Bernstein *et al.*, 2008; Bowden, 2008), reactor power (Bernstein *et al.*, 2008), and the rate change due to fuel burnup (Bowden *et al.*, 2009); see Fig. 3. This group also developed a more optimized homogeneous GdLS detector design (Classen *et al.*, 2015) with improved detection efficiency and energy resolution.

The Nucifer Collaboration (Boireau *et al.*, 2016), based in France, performed a monitoring demonstration at the 70 MW_{th} Osiris research reactor. The aim was to develop a detection system suitable for operation within a research reactor building. Considerable effort went into the certification process that allowed the detector to operate within 7 m of a reactor core. The design was based on 0.8 tons of GdLS in a single vessel. Significant shielding was required to suppress reactor-correlated γ-ray backgrounds. At the relatively modest

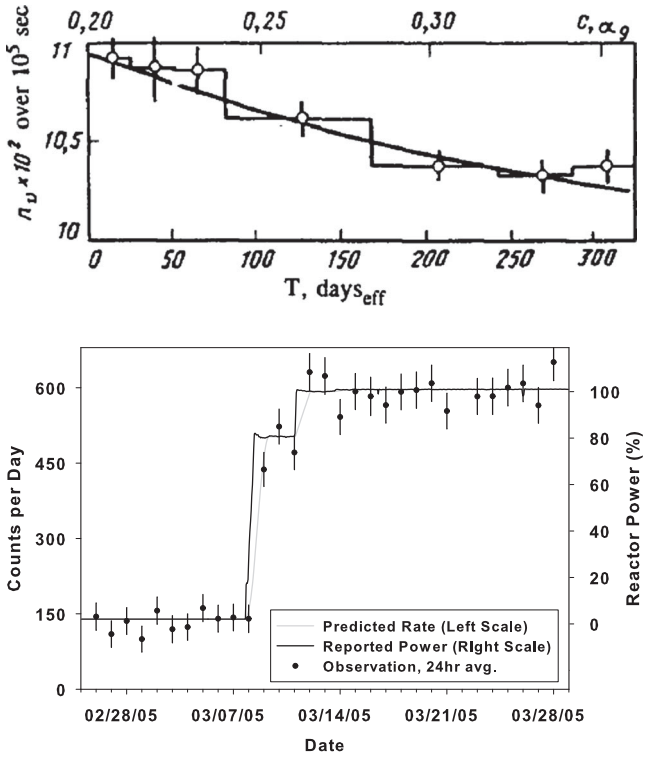

FIG. 3. (Top) Measurement of fuel burnup at Rovno. The detected reactor antineutrino rate decreases over an observation period of 300 days as production and burning of ^{239}Pu reduces the emitted antineutrino flux. From Klimov *et al.*, 1994. (Bottom) Observation of reactor start-up at SONGS. The correlated event rate tracks the change in reactor power at start-up, where the events measured at zero power are due to the background. From Bowden, 2008.

overburden of 12 mwe,[6] the use of PSD[7]capable GdLS was important for suppression of cosmogenic correlated neutron backgrounds. Recording almost 300 IBD interactions per day with S:B = 1:4, Nucifer was able to follow the operation state and power level of the Osiris reactor.

Subsequent efforts addressed the desire to operate detectors on the Earth's surface without cosmic-ray attenuating overburden, since this enables deployment in a much broader range of locations. Particle type identification and interaction localization capabilities are key design features that have been developed to address the much greater background encountered at the Earth's surface. Examples of such techniques include segmentation, which provides position resolution roughly equivalent to the segment pitch in compact detectors, and neutron-capture identification based on event topology and/or incorporation of ^{6}Li, which yields a tightly localized

[6]The acronym mwe is short for meter water equivalent and allows one to express overburden independent of the specific rock or soil composition.

[7]PSD stands for pulse shape discrimination, which allows one to distinguish particles based on their mean energy loss per traveled distance dE/dx. Particles with a high dE/dx tend to produce a broader light emission pulse than particles with small dE/dx, such as beta rays (Brooks, 1959).

signal upon neutron capture. The event localization capability provided by segmentation allows selections based on spatial correlations, in addition to the timing correlation supplied by the IBD reaction. For example, the use of event location information to require a spatial coincidence between the prompt and delayed components of an IBD event candidate is effective at suppressing random temporal coincidences of singles backgrounds. The spatial pattern (topology) of energy depositions within the prompt and delayed components themselves can also be of use. Examples include attempts to preferentially select deposition patterns corresponding to IBD positrons (primary positron ionization energy loss and the Compton scattering of the resulting 511 keV annihilation γ rays) and neutron captures on Gd (Compton scattering of multiple MeV-scale γ rays).

The PANDA project (Kuroda *et al.*, 2012; Oguri *et al.*, 2014) realized several generations of detectors based on an heterogeneous arrangement of plastic scintillator (PS) and Gd coated sheets. Operation of the PANDA-360 prototype at a reactor in Japan without overburden provided a low significance hint of reactor state determination with S:B of less than 1:15 (Oguri *et al.*, 2014). Similar approaches have been pursued by groups in India (Mulmule *et al.*, 2018) and the United Kingdom (Carroll *et al.*, 2018).

The group responsible for SONGS1 developed an approach that provides a distinct neutron-capture identification signal using ^{6}LiZnS neutron-capture screens (Kiff *et al.*, 2011). When layered between segmented PS bars, highly localized neutron captures on ^{6}Li could be identified via the slow ZnS scintillation time constant using PSD. This approach strongly suppresses background events due to spallation processes that produce multiple neutrons that can enter a detector and be captured with a time correlation structure similar to IBD (Bowden, Sweany, and Dazeley, 2012) that are difficult to identify in detectors that use Gd or other γ-ray emitting neutron-capture agents, while also reducing accidental coincidence backgrounds. A small prototype deployed in a 20 ft ISO shipping container at SONGS without overburden did not have sufficient sensitivity to observe neutrinos, but did demonstrate powerful background reduction (Reyna *et al.*, 2012). The use of wavelength shifting (WLS) materials to efficiently transport ^{6}LiZnS scintillation to photosensors at the edges of a heterogeneous detector arrangement, first developed for neutron scattering experiments (Eijk, van, Bessière, and Dorenbos, 2004), is an important element of this approach.

As discussed in Sec. VI, demonstrations of far-field capabilities beyond 10 km or so require kiloton-scale detectors, with target masses increasing to the megaton scale beyond ∼100–200 km. The first dedicated far-field demonstration of reactor monitoring was initiated by the US-UK WATCHMAN Collaboration (Askins *et al.*, 2015). WATCHMAN is an acronym for the water Cherenkov monitor of antineutrinos, a Gd-doped water Cerenkov detector with a fiducial mass of 1000 tons, located in an underground site 25 km from a dual-reactor complex in the UK. The WATCHMAN Collaboration is currently planning for the start of data-taking operations in approximately 2025.

C. Return to fundamental physics with near-field reactor observations

In recent years, searches for new physics in the neutrino sector have brought basic science attention back to near-field reactor observations. In 2011, recalculations of reactor neutrino fluxes were found to be significantly higher than the ensemble of observations (Huber, 2011; Mention *et al.*, 2011; Mueller *et al.*, 2011). Among other possibilities, this discrepancy could be explained by the existence of a sterile neutrino, a neutral fermion with even weaker couplings to matter than the standard model neutrinos or by deficiencies in the nuclear data and methods used to predict the reactor antineutrino flux. Indeed, the discrepancy between recent precision energy spectrum measurements (F. P. An *et al.*, 2016; Choi *et al.*, 2016) and prediction, most prominent near 5 MeV, is a strong indication that such deficiencies exist.

A wide variety of detector designs has been proposed to test the sterile neutrino hypothesis. Many of these detectors must operate at or near the surface with limited cosmic-ray attenuating overburden due to the configuration of the host reactor facilities and are designed to provide good energy resolution, detection efficiency, and/or background rejection. Here we detail some effort of particular relevance to reactor monitoring applications.

The NEOS experiment (Ko *et al.*, 2017) operates in a below-ground location similar to SONGS1. Using a 1-ton GdLS target and PSD for background suppression, a signal-to-background ratio of 20 and event rate of ∼2000 IBD interactions per day are achieved. In the context of near-field reactor monitoring, this device provides high statistics for rapid determination of reactor status, power level, and measurement of the reactor antineutrino energy spectrum. NEOS represents an excellent example of what can be achieved using a modern GdLS material in a location with 20 mwe or more overburden. The STEREO (Almazán *et al.*, 2018) and Neutrino-4 (Serebrov *et al.*, 2019) experiments have also successfully performed reactor antineutrino measurements at research reactors using GdLS target material. In both cases, a modest overburden of the order of 10 mwe was available. DANSS (Alekseev *et al.*, 2018) has also achieved a high reactor antineutrino counting rate using a heterogeneous detector composed of PS bars and Gd coated sheets. Operating in a location beneath a power reactor core, DANSS enjoys high antineutrino flux and ∼50 mwe overburden, providing sufficient sensitivity to observe small flux variations due to reactor operations (Alekseev *et al.*, 2019).

The PROSPECT experiment (Ashenfelter *et al.*, 2016) has made a significant advance by performing the first demonstration of on-surface reactor antineutrino detection with S:B ∼ 1 (Fig. 4), this being achieved at a research reactor facility with less than 1 mwe overburden (Ashenfelter *et al.*, 2018a). This result can now serve as a benchmark for reactor monitoring use cases involving on-surface detector deployment (Carr *et al.*, 2019). The PROSPECT detector design incorporates multiple capabilities that combine to efficiently reject cosmogenic backgrounds. The use of 4 tons of PSD-capable ^{6}Li-doped LS (LiLS) provides fast neutron and neutron-capture identification, while a 2D segmented geometry (14.5 cm pitch) provides event localization and topology.

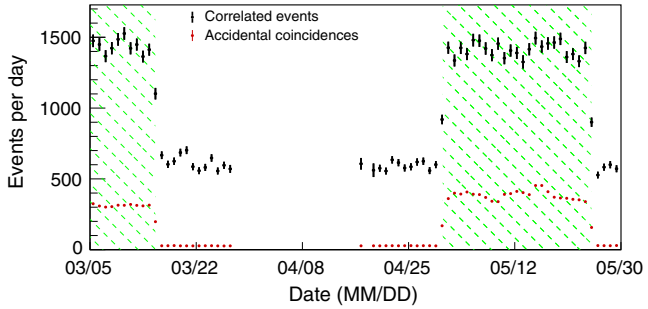

FIG. 4. On-surface measurement of the reactor operational state by PROSPECT with less than 1 mwe of overburden. Green (gray) shaded periods correspond to full power operation of the host reactor, with the correlated event excess relative to reactor off periods being due to detection of reactor antineutrinos. From Ashenfelter *et al.*, 2018a.

An emphasis on efficient, uniform light collection results in very good energy resolution for an organic scintillator detector (Ashenfelter *et al.*, 2018b), which has been utilized in a measurement of the ^{235}U reactor antineutrino energy spectrum (Ashenfelter *et al.*, 2019). Initial background predictions for PROSPECT (Ashenfelter *et al.*, 2016) are in good agreement with the data reported by Ashenfelter *et al.* (2018a), including observation of spectral features due to multiple neutron and neutron inelastic processes.

Several other approaches focus on more finely grained segmentation than PROSPECT. SoLid was among the first near-field reactor efforts to propose and realize finer-grained three-dimensional segmentation as a background rejection strategy (Abreu *et al.*, 2018a, 2018b). This detection concept combines ^{6}LiZnS neutron-capture sheets, 5 cm cubes of PS, and WLS optical fibers, providing 3D topological information and neutron-capture identification. SoLid has collected reactor data and analysis is ongoing to determine the extent to which event topology information obtained from relatively fine-grained 3D segmentation can be used to reject fast neutron backgrounds in a ton-scale detector. The goal is to identify positronlike event topologies including spatially isolated depositions from 511 keV annihilation gamma rays.

NuLat uses a light collection arrangement known as the Raghavan Optical Lattice (ROL) to obtain fine-grained 3D segmentation (also ~5 cm pitch) and efficient light collection (Lane *et al.*, 2015). The use of homogeneous ^{6}Li-doped materials in combination with the ROL promises access to all proposed particle identification methods simultaneously—fast neutron recoil PSD, neutron-capture PSD, and fine-grained topological information—and therefore should have excellent background rejection. The current availability and optical performance of ^{6}Li doped PSD-capable plastic scintillators has limited the extent to which the concept has been demonstrated to date.

Inspired by the SoLid, SNL and LLNL, and NuLat segmented efforts, CHANDLER uses ^{6}LiZnS screens, wavelength shifting plastic scintillator, and an ROL to provide fine-grained topology information, a distinct neutron-capture tag, and good optical collection and energy resolution compared to SoLid. In contrast to NuLat, the CHANDLER concept can be realized with materials that are readily available from commercial vendors. As with SoLid, the ability to identify and reject background is based on event topology information obtained from relatively fine-grained segmentation in combination with a distinct neutron-capture tag. CHANDLER reports IBD detection including the spectrum from several months operation without overburden at a 2900 MW_{th} pressurized water reactor using an 80 kg miniCHANDLER prototype (Haghighat *et al.*, 2018). CHANDLER is among the efforts to have demonstrated a main advantage of solid plastic detectors: the miniCHANLDER prototype is mounted inside a road-legal trailer, it can be driven to the deployment site, and data taking can start within hours of deployment.

V. APPLICATIONS TO KNOWN REACTORS: FISSILE MATERIAL PRODUCTION MONITORING

A. Existing approaches

The IAEA implements a variety of technical measures to verify a state is in compliance with its safeguards agreements. Safeguards are primarily designed to detect the diversion of nuclear material from declared facilities, undeclared processing or production of nuclear materials at declared facilities, and undeclared facilities processing or producing nuclear material. The IAEA implements safeguards using a combination of nuclear material accountancy, nondestructive and destructive measurements, and containment and surveillance.

Measurements of nuclear material confirm the declared mass and composition of the material, typically by employing nondestructive measurements, e.g., measuring the weight of a uranium sample using a scale and measuring its isotopic composition using gamma spectroscopy. Destructive measurements are employed when necessary, e.g., measuring the isotopic composition of a solution of dissolved irradiated fuel using mass spectrometry. Measurements also verify the declared operation of a process, e.g., by measuring the flow rate of UF_6 in a gas centrifuge plant. Furthermore, environmental sampling at predesignated locations within declared facilities is frequently applied to detect the presence of undeclared materials or declared materials in anomalous locations, which can be indicative of diversion, undeclared processing. Wide-area sampling, i.e., outside of declared facilities, is permitted under the Additional Protocol to uncover undeclared facilities; however, it is not approved as a routine inspection tool and usually reserved for cases where a specific concern exists.

Finally, containment and surveillance are the key technologies to detect undeclared access to and/or movement of nuclear material. Containment is implemented using tamper-indicating seals applied to nuclear material containers and process controls; attempts to access or move the nuclear material, or change the operation of a process, would be detected if the integrity of seals were compromised. Surveillance is primarily implemented using cameras to observe material balance areas and process controls. Currently, most safeguard surveillance systems do not provide real-time remote monitoring; however, the IAEA is working to transition its surveillance systems to provide real-time remote monitoring of many facilities in the near future.

The declared burnup of spent fuel is primarily verified using accountancy of the fresh and irradiated fuel and nondestructive analysis of the fresh and irradiated fuel. Nondestructive analysis of the fresh fuel serves to verify its declared mass and enrichment, which is accomplished by relatively simple weight and gamma spectroscopic measurements. However, nondestructive analysis of the irradiated fuel does not yield a direct measurement of the fuel's isotopic composition, including the fuel's residual uranium content and the plutonium bred in the fuel during irradiation, because gamma and neutron emissions by fission products in the fuel mask radiation emissions from the uranium and plutonium isotopes.

Radiation measurements of SNF are used to confirm that it is consistent with the declared initial enrichment, burnup, and cooling time. The most widely used technique is based on measuring the Cerenkov radiation emanating from SNF within the water of the spent fuel pond. This is accomplished using the so-called Cerenkov viewing device (CVD) (Chen, Gerwing, and Lewis, 2001), which essentially just confirms that the SNF is present and exceeds a certain level of overall radioactivity. The advantages of the CVD are that it is fast, it does not require fuel movement, and it does not get into contact with the pool water. The fission and/or activation product content of the fuel can be measured using gamma spectroscopy and/or neutron coincidence counting, but these techniques are rarely employed (IAEA, 2011). Except in the case of a few research reactors, typically with a thermal power in excess of 25 MW, safeguards do not implement real-time monitoring of reactor operations. For those exceptional reactors power is measured by using the advanced thermohydraulic power monitor (Zendel *et al.*, 2011), where the flow rate of coolant and temperature rise across the reactor are measured. For SNF in dry storage the default technologies are tamper-indicating seals and surveillance. The majority of nuclear reactors has a significant amount of fertile material, i.e., material that under neutron irradiation can become fissile, present in the reactor core; in power reactors uranium-238 is the most important of those. As a consequence, these reactors produce some fissile material, notably plutonium-239, during operation. The amount and quality of plutonium produced is a function of the total burnup and the initial fuel enrichment and composition: for a typical 3 GW_{th} pressurized water reactor a plutonium production rate of 100–200 kg per year is not unusual. Therefore, verifying burnup, enrichment, and fuel composition is an important part of safeguards. In particular, a willful misdeclaration of any of those quantities would allow for the production of excess plutonium (or a more weapons-usable grade) or to overstate the amount of plutonium which is consumed. The latter is critical for international agreements to reduce the stockpile of fissile material.

Real-time remote monitoring of nuclear reactor operations has been demonstrated using satellite and aerial imagery of heat signatures emanating from the reactor. The reactor's thermal output, in terms of either its injection of hot water into a reservoir or its emission of warm air from its cooling towers, can reveal the on or off state of the reactor and can be correlated to the reactor's operating power (Garrett, Casterline, and Salvaggio, 2010; Lee and Garrett, 2015). At shorter ranges (e.g., hundreds of meters), sky shine (gammas scattering in the air above a reactor containment building) can also reveal the on or off state of the reactor (Wahl *et al.*, 2014).

B. Neutrino-based approaches

Section III.C contains a description of how neutrino emissions carry information about reactor power levels and fuel contents. This information, collected in real time, could complement existing reactor monitoring techniques. The basic neutrino observables are neutrino rate, neutrino energy spectrum, and time evolution of neutrino spectrum and rate. These observables in turn allow one, at least in principle, to measure the fission rates $f_I(t)$ and thus, also reactor power. The rate at which the fission rate $f_I(t)$ changes with time is indicative of the initial fuel enrichment. All neutrino observations are measuring the neutrino emission from the entire reactor core and thus any inferred quantity always represents a core average. That is, neutrino-based technology provides a form of bulk accountancy, whereas current procedures are mostly providing item accountancy. In the context of some advanced reactor designs, like molten salt reactors, item accountancy will not be possible, providing additional motivation for neutrino-based approaches.

Reactors with a high neutron flux density will produce more fissions per unit mass of the fissile nuclide. This relationship connects neutrino measurements to the core fissile inventory. Smaller reactors contain less plutonium and thus it is easier to achieve an absolute goal, like detection of 1 SQ. This indicates that commercial, multi-GW light water-moderated reactors are a challenging target for neutrino safeguards relative to the IAEA goals. However, even for those reactors, neutrino safeguards can provide a 1%–2% core-wide plutonium inventory, which exceeds the accuracy of any other practical approach, a capability which would become relevant in the context of the FMCT. On the other hand, for typical plutonium production reactors, research reactors, and small modular reactors neutrinos can meet the IAEA goals in terms of both quantity and timeliness of the result.

One case to mention is the so-called Nth-month scenario: The reactor in question is a heavy-water moderated, natural uranium fueled 40 MW_{th} reactor, which produces about 10 kg of weapons-grade plutonium per full power equivalent year. Assume the reactor is running at nominal power and that there is full safeguards access for $N-1$ months. In the Nth month, there is a reactor shutdown followed by a lapse in safeguards access. In month $N+1$ reactor operation and safeguards access resume, i.e., the inspectors are confronted with a closed reactor core and a running reactor. Furthermore, if we take $N=10$, then the core just prior to shutdown would contain 8 kg weapons-grade plutonium. This is a specific example for a loss of continuity of knowledge (CoK) incident. Loss of CoK incidents have been reported and, in particular, seem to occur in states which are new to or reentering into the safeguards regime. Conventional means of safeguards are largely based on item accountancy and very few actual measurements are ever performed, so CoK is one of the central pillars. Experience shows that recovery of CoK in a reactor setting is difficult and would be expensive and highly intrusive (Christensen, Huber, and Jaffke, 2015). In Fig. 5 the

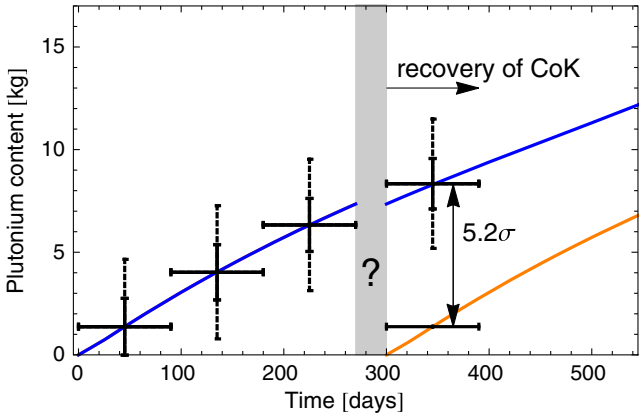

FIG. 5. The 1σ accuracy for the determination of the plutonium content of the reactor as a function of time in the reactor cycle. The data-taking period is 90 days each. Dashed error bars indicate the accuracy from a fit to the plutonium fission rate f_{Pu}, whereas the solid error bars show the result of a fit constrained by a burnup model. The blue (dark) line indicates operation without refueling and the orange (light) line indicates operation with a refueling after 270 days. From Christensen *et al.*, 2014.

plutonium mass sensitivity obtained by a neutrino measurement for the *N*th-month scenario is shown.

A 90-day postshutdown measurement provides a plutonium inventory with an accuracy of 1.2 kg or the question of whether the core has been swapped can be answered with 90% confidence within 7 days. This example is based on a 5 ton detector at 20 m standoff. It is important to note that despite Fig. 5 showing data for all four measurement periods, the conclusion about the core state really is obtained in each 90 day period independently of any other 90 day period. In this scenario, neutrino measurements allow restoration of the CoK in a short period of time and in an entirely nonintrusive manner.

In this example the assumption was that the reactor would be running at nominal power, but also in the case of the reactor remaining shut down there are usable neutrino signatures. These residual signatures arise from four fission fragment nuclides which have half-lives between 100 days and 28 years. As a result, a reactor core emits neutrinos even after shutdown. For a time after shutdown between 30 and 90 days, there are 1–2 events per day stemming from the afterglow. Detection of such a low event rate requires a detector with exceptional background suppression, but given such a detector these events could be used to infer the presence of an irradiated core with a certain minimum burnup.

For the same reactor and detector combinations, a different fueling scheme was examined. Assume this reactor, at the same power, was converted to run on 3.5% enriched uranium fuel using a light water moderator (Willig, Futsaether, and Kippe, 2012). Such a scheme would greatly reduce plutonium production and extend the fuel cycle. The key to the neutrino measurement in this case is that the fission rates f_I change significantly faster in a natural uranium fueled reactor than they do in an enriched core. A measurement of those fission rate changes, called differential burnup analysis, allows one to distinguish the two fueling schemes within about 180 days (Christensen *et al.*, 2014).

Burnup also can be determined through a continuous neutrino measurement of reactor power. The evolution of the total count rate distinguishes different fuel loadings in a light water reactor: in a LEU core the rate is expected to decline with time, whereas in a mixed oxide (MOX) core the rate increases or stays nearly constant. The rate-based approach was studied by Bernstein, Bowden, and Erickson (2018) based on highly detailed reactor physics simulations for various MOX fueling schemes. A spectral neutrino measurement allows determination of the fission rates f_I and thus direct confirmation of the isotopic composition and changes thereof which are expected for a certain burnup (Jaffke and Huber, 2017). The corollary to those studies is that neutrino monitoring can distinguish MOX from LEU and mixed cores and provide an indication whether reactor-grade or weapons-grade plutonium is put into the reactor. Neutrino measurements also can provide assurance that disposition goals in terms of total burnup and isotopic degradation of weapons-grade plutonium have been met.

Disposition of plutonium in fast breeder reactors has been proposed and in a broader context, there are fuel cycles, like a thorium-based one, where fast breeders are an integral part. A breeder reactor is a type of reactor which produces more fissile material than it consumes and typically is based on the use of fast neutrons. Breeder reactors use driver fuel to generate neutrons and breeding blankets made of fertile material, e.g., natural uranium or thorium. Because of their use of fast neutrons they can use pure or nearly pure plutonium as driver fuel, whereas in a thermal reactor only relatively limited amounts of plutonium can be added to the uranium fuel, so-called mixed oxide fuel. A breeder reactor run without a blanket of fertile material is a net user of fissile material and if the driver fuel were made of plutonium, significant quantities of plutonium can be consumed and thus destroyed. Safeguarding breeder reactors is complicated by the variable breeding ratio resulting from the presence or absence of a breeding blanket of fertile material. Assessing the presence of a blanket is hard because there are relatively few fissions that occur in the blanket, yet, at the same time it is placed right next to a vigorously fissioning core. Effectively, the core fissions drown out any radiation signatures from the blanket. However, there is a unique neutrino signature from breeding:

$$^{238}\mathrm{U} + n \rightarrow {}^{239}\mathrm{U} \xrightarrow{\beta^-} {}^{239}\mathrm{Np} \xrightarrow{\beta^-} {}^{239}\mathrm{Pu}, \tag{9}$$

where the two beta decays have short half-lives of 24 m and 2.4 days and end-point energies of 1.26 and 0.72 MeV, respectively. Similar signatures exist in a thorium-based fuel cycle. The resulting antineutrinos are below the IBD threshold and hence invisible to the usual neutrino detectors. It may be possible to detect them in CEνNS detectors. A detailed study was performed by Cogswell and Huber (2016) and they found that detectors of moderate size, several tens of kilograms, could reliably detect the presence of a breeding blanket at a standoff of 25 m.

VI. APPLICATIONS TO UNDECLARED REACTORS: REACTOR DISCOVERY AND EXCLUSION

A. Existing approaches

Historically, there are numerous cases of reactor construction and operation being discovered by intelligence gathering (Richelson, 2007). Technological approaches to discovery or exclusion of reactors have been more limited. Technological methods that may be useful for remote monitoring and discovery of reactors include thermal and visible wavelength satellite or aerial surveillance and monitoring of xenon, krypton, and other radio nuclides in the atmosphere far from their point of origin.

Roughly speaking, a reactor fissions a kilogram of material per GW day of heat produced. The heat generated by fission can be rejected into the air via cooling towers or into a lake, river, or the ocean via cooling water. These thermal signatures can in principle be detected from space or airborne thermal-infrared cameras (Hafemeister, 1989), or in the winter, by surface ice melting downstream from a reactor cooling water outlet. Satellite surveillance can observe construction activities, and in the case of thermal imagery, it can provide a rough estimate of power output for some reactor designs. Disadvantages of this approach are the need for cueing information that is extraneous information sources that enable the satellite surveillance to focus the search on a specific area due to its limited field of view, the dependence on weather, the qualitative nature of the power estimates, and susceptibility to masking or dissipation of the thermal signature.

Noble gases and other radioactive gases from fission are created in operating reactors. These can escape through cracks in the outer layers of fuel rods, and they may ultimately be released to the atmosphere. The detectability of noble gases released from reactors depends on the integrity of the fuel and cladding, pathways within the reactor complex to the atmosphere, and the weather conditions along the path from the reactor to the radio-nuclide detection apparatus (Saey, 2007). This approach to reactor discovery can also suffer from confounding signals arising from radio-nuclide release from other nuclear facilities, such as reprocessing plants or radioisotope production facilities.

Given the relatively limited set of tools available for remote reactor discovery, exclusion, and monitoring, antineutrino-based methods offer unique features that may be of use in current or future monitoring regimes.

B. Neutrino-based approaches

Neutrino-based techniques offer significant advantages: persistence; the ability to detect or exclude reactor activity in a wide geographical region without external cueing information; insensitivity to weather, shielding, and other environmental factors; the potential to place constraints on, or directly measure, the operational status and total thermal power of the reactor, and thereby estimate the maximum possible rate of plutonium production in the discovered reactor.

As standoff distances increase from the near-field regime, the event rate that can be practically achieved drops, even in large detectors, from tens or hundreds of events per day to a few events per day, week, or month. Timely direct measurement of fissile content becomes difficult or impossible, simply due to the small event samples obtainable in reasonable integration times. Still it may be possible to discover, or exclude the existence of, undeclared reactors in regions surrounding the detector location. In addition, constraints can be placed on the total power output of a known reactor, or a set of known reactors, over periods of months, providing an upper bound on fissile material production. If backgrounds are sufficiently well understood through simulation and calibration, the existence of an undeclared reactor can in principle be discovered by looking for a signal above the known background. If backgrounds must be measured in place, then only a sufficiently large change in the reactor power can be observed, manifested as a deviation from a stable background.

Prediction of backgrounds is a significant challenge for these types of experiments. Ambient radioactivity levels from the detection medium, detector materials, and surrounding rock must be measured and incorporated into simulations. As a result, screening campaigns for all construction materials are a common practice for underground particle detectors. Modeling is more complex for muogenic backgrounds, including neutrons and long-lived radio nuclides. A widely used model for muogenic neutron backgrounds is that of Mei and Hime (2006), while muon tranport codes such as MUSIC and MUSUN (Kudryavtsev, 2009) are used to propagate muons to great depths underground and study angular dependence.

Aside from questions of modeling backgrounds, there are several limitations on neutrino-based approaches: the smallness of the IBD cross section; backgrounds of real antineutrinos from the hundreds of existing civilian power reactors worldwide; and persistence of cosmic-ray induced backgrounds, which for large detectors can be reduced only by underground deployment.

We use a 50 MW_{th} reactor as a "standard candle," this power being roughly typical of the scale of plutonium production reactors. Excluding the presence of such a reactor within 1 yr with 95% confidence at 1000 km standoff requires a 335 kt fiducial mass water-based detector. This mass estimate assumes a 100% efficient detector above an antineutrino energy threshold of 3.26 MeV (imposed to remove geoantineutrino backgrounds, as described later), no observed events, and a Poisson-distributed background consistent with zero. With these assumptions, the 335 kt detector would have been 95% likely to have observed greater than zero events with three signal events expected on average. Clearly, the smallness of the IBD cross section is a challenge.

Constraints imposed by other backgrounds further increase the detector size or dwell time. In order of increasing standoff one needs to deal with different types of background. Up to 20 km the dominant backgrounds are accidentals from local radioactivity, fast neutrons, and long-lived muogenic radio nuclides. These can be controlled by locating the detector underground and by careful material selection. Additional research is needed to determine the degree to which these backgrounds can be suppressed in 100 kt and larger detectors and studies of achievable sensitivities have been performed (Lasserre *et al.*, 2010).

At larger standoffs, geoneutrinos stemming from uranium and thorium decays in the Earth (Krauss, Glashow, and

TABLE II. For three representative reactor antineutrino background levels, this shows the detector fiducial mass in kilotons and dwell time in years required to achieve 3σ sensitivity to the presence of a 50 MW_{th} reactor. The three background categories correspond to the actual reactor and geoneutrino backgrounds at the existing Andes, Baksan, and Frejus underground laboratories (Barna and Dye, 2015), with 170, 2080, and 28 000 background events per year and 100 kt detector mass. The data are formatted as mass [kt] × dwell time [years]. Blank cells indicate that the dwell time is greater than 1 yr, or the detector mass is greater than 1 Mt. Neutrino oscillations are accounted for and an energy cut to largely remove geoneutrinos is applied.

Distance (km)	10	20	50	100	200
Low background	1×0.08	1×0.4	10×1	100×1	1000×0.8
Medium background	1×0.1	1×0.7	100×0.7	1000×1	
High background	1×0.3	5×1	1000×0.9		

Schramm, 1984, ; Bellini *et al.*, 2013) become non-negligible. Since their energies do not exceed 3.26 MeV an energy cut on the reconstructed positron spectrum can remove this background, although in many detectors, upward fluctuations of the apparent reconstructed energy can contaminate the signal region.

At standoffs of 100 km or more, reactor antineutrino backgrounds become a limiting factor. These backgrounds are the greatest concern in monitoring contexts, since they cannot be removed except by reconstructing the direction of the incident antineutrino, which is challenging to accomplish for IBD events. Less well measured but potentially also important are IBD-like events induced by high energy atmospheric neutrinos and antineutrinos, including both charged and neutral current channels on oxygen (Langanke, Vogel, and Kolbe, 1996). For the largest detectors contemplated in this Colloquium, at the megaton scale, the as-yet-unmeasured but long-predicted diffuse supernova antineutrinos may become a limiting background (Beacom, 2010).

The summed background contributions from all of the world's reactors at any point on Earth can be estimated to a precision of about 5% (Barna and Dye, 2015; Usman *et al.*, 2015). This integrated background contribution varies by a factor of about 30 from the northern to the southern hemisphere, ranging from a high of 2000 to a low of ∼65 events per 100 kt of water per year (Lasserre *et al.*, 2010). This background is irreducible, unless event-by-event measurements of the neutrino direction become possible. Therefore, the limit in sensitivity is set by the global reactor neutrino background, where we distinguish regions with low, medium, and high reactor neutrino backgrounds as shown in Table II. The conclusion from this simple exercise is that standoff distances beyond 200 km will require event-by-event measurements of the neutrino direction (Jocher *et al.*, 2013).

C. Technology options

Water Cerenkov and scintillation detectors are the only viable target media for the construction of large-scale (kiloton and above) antineutrino detectors implied by Table II. Within tens of kilometers, few-kiloton detectors suffice to achieve basic monitoring goals, e.g., KamLAND (Eguchi *et al.*, 2003) and JUNO (F. An *et al.*, 2016), and these could be based on a liquid scintillator. To build the larger, 100 kt or megaton size, detectors for use in the far-field, water-based technologies appear promising. The 50 kt Super-Kamiokande water Cerenkov detector has already demonstrated sensitivity to MeV-scale (solar) neutrinos (Renshaw *et al.*, 2014). However, in pure water detectors, neutrinos and antineutrinos are indistinguishable. This greatly complicates the detection of antineutrinos, because the neutrino or antineutrino signal consists only of a single flash of light induced by the neutrino or antineutrino. For that signal, backgrounds consist of the full gamut of sources that can induce MeV-scale single events, including gamma rays from radioactive contaminants in the target medium and detector materials, cosmogenic muons and neutrons, and muogenic radio nuclides. Solar and other neutrinos are also of course a background to antineutrinos in such detectors. Conversely, if the neutron from IBD interactions [see Eq. (5)] can be tagged efficiently, the presence of this signal in close time coincidence with that induced by the positron permits suppression of backgrounds by 3 orders of magnitude or more compared to a search for a single MeV-scale energy deposition.

To break the degeneracy of antineutrinos and neutrinos, and permit efficient and unambiguous detection of MeV-scale antineutrinos, researchers have proposed to add gadolinium to water (Bernstein, West, and Gupta, 2001; Beacom and Vagins, 2004) at roughly the part per thousand level by weight. Gadolinium, an efficient neutron-capture element, greatly improves the efficiency for detection of the final state neutron in the IBD process.

A 200-ton engineering demonstration of gadolinium-doped water technology was achieved by the EGADS group (Xu, 2016). The experiment demonstrated the compatibility of standard materials with gadolinium-doped water and showed that the effective attenuation length of Cerenkov light in gadolinium-doped water remained high, a key consideration for the construction of large-scale detectors. In part based on this research, the Super-Kamiokande Collaboration announced (Castelvecchi, 2019) that it would add gadolinium to the detector, primarily in an effort to detect diffuse supernova antineutrinos.

In 2018, the dedicated WATCHMAN experiment was launched (NYT, 2018) to investigate the viability and scalability of gadolinium-doped water as a tool for reactor antineutrino detection in nonproliferation contexts. It will be constructed in the Boulby mine in northern England and will measure neutrinos emitted by the Hartlepool nuclear reactor complex, 25 km distant.

In order to breach the 200 km limit for remote sensitivity implied by Table II, directional reconstruction methods on an event-by-event basis will be needed for reactor antineutrinos. In the IBD reaction the momentum of the neutrino is carried

by the neutron and hence the neutron momentum would need to be reconstructed, a daunting task in a megaton-scale detector. In the neutrino-electron scattering reaction, the scattered electron carries the momentum of the neutrino, but the expected event rate per unit mass for hydrogenous targets is approximately 5 times lower than for IBD (Dye, 2017).

In spite of the difficulties, the high value of directional reconstruction for background suppression motivates continued investigations in this area. Examples of directional concepts for IBD and neutrino-electron scattering, respectively, have been given by Safdi and Suerfu (2015) and Hellfeld *et al.* (2017).

VII. APPLICATIONS TO SPENT FUEL AND REPROCESSING WASTE: DISCOVERY AND MONITORING

A. Existing approaches

At present, compliance with safeguards agreements is based on observations made before a storage cask or underground repository is closed and relies upon the integrity of seals and remotely monitored cameras to verify that these closed volumes were not opened between inspector visits. However, seals can be opened and closed without detection (Johnston, Garcia, and Pacheco, 1983) and cameras can be unplugged or blocked, intentionally or inadvertently. It therefore would be desirable to verify that the situation inside a sealed container or repository is as expected without having to open it.

It is challenging to verify the plutonium content of SNF using nondestructive measurements. IAEA SNF safeguards therefore employ radiation measurements to confirm that specific characteristics (termed attributes) of the fuel are consistent with the declared initial enrichment, cooling time, and burnup. These radiation measurements are typically confined to take place during wet storage in a fuel pond and are performed using a combination of gamma spectroscopy, gross neutron counting, neutron coincidence counting, and Cerenkov imaging, where the latter is the most commonly used. In principle, this combination allows one to confirm gamma and neutron emissions expected from characteristic nuclides and Cerenkov light indicating that all individual fuel rods in the assembly are present; see also Sec. V.A.

B. Neutrino-based approaches

Dry storage of some form is the final destination for almost all SNF. The bulk of SNF is currently in wet storage, but in the aftermath of the Fukushima Daichi nuclear accident the associated safety ramifications became all too obvious (NAS, 2016). These safety concerns combined with eventual decommissioning of nuclear power plants will lead to a significant increase of the amount and fraction of all SNF in dry storage; see, for instance, U.S. Government Accountability Office (2014). For the verification of SNF in dry-cask storage facilities, neutrino monitoring could be an option if the cost were affordable within the IAEA budget. SNF and reprocessing waste (RW) are intensely radioactive and the bulk of nuclear decays occurs via beta decay, thus, both constitute neutrino sources. For neutrino detection based on IBD, however, only neutrinos above the IBD threshold of 1.8 MeV are visible. Sargent's rule states that beta decay rates are proportional to Q^5, where Q is the endpoint energy in the neutrino spectrum; thus beta emitters with an endpoint above the IBD threshold tend to be very short lived (Sargent, 1933). One year after discharge from the reactor, all detectable neutrinos stem from only three pairs of nuclides: ^{90}Sr/Y, ^{144}Ce/Pr, and ^{106}Ru/Rh. The reason they appear in pairs is related to Sargent's rule: the first decay in the pair is a low-energy, and hence relatively long-lived decay, whereas the second decay is of higher energy and therefore short lived. For source material older than a few years, only the ^{90}Sr/Y decay chain, with a half-life of about 29 years, is relevant. This also implies that for any SNF/RW produced to date, only about 2.6 half-lives have elapsed, and this emission is still at 16% of its original value. Fortunately, ^{90}Sr has a high cumulative fission yield[8] of 1%–5%. In reprocessing, ^{90}Sr will end up in the waste stream and thus RW is a significant neutrino source for long periods of time.

In most countries, the bulk of SNF produced in commercial nuclear power plants eventually ends up in dry storage casks. The rate of neutrino events per ton of fiducial detector mass and per metric ton of uranium (MTU) of source mass is, assuming a burnup of 45 GW d MTU^{-1} (Brdar, Huber, and Kopp, 2017)

$$N_\nu = 5.17\ \mathrm{yr}^{-1}\,\mathrm{ton}^{-1}\,\mathrm{MTU}^{-1} \times (10\ \mathrm{m}/L)^2, \qquad (10)$$

where L is the distance between the source and the detector (both treated as pointlike). Typically, these storage facilities are close to an operating nuclear reactor complex and thus there will an irreducible background of neutrinos coming from the reactor. This size of this background can be accurately measured in the same neutrino detector used for the SNF signal. Because of the high energy of the reactor neutrinos as compared to the SNF neutrinos the two components can be disentangled and only the statistical uncertainty from background subtraction remains. A real existing dry storage facility is taken as an example and it is found that a change of inventory by as little as 3% can be detected with exposures in the range of 20–80 ton years at a standoff of up to 50 m (Brdar, Huber, and Kopp, 2017). In this analysis the assumption is made that cosmogenic and other non-neutrino backgrounds can be reduced to negligible levels.

Eventually, most nations plan to store SNF in long-term geological repositories. Given the large amount of SNF at such a site, 10^4–10^5 MTU, the resulting neutrino signal will be large, tens of events per year, and 1 ton at the kilometer scale standoff. In particular, after closure of the repository, neutrinos will be the only detectable radiation signature. Following the analysis by Brdar, Huber, and Kopp (2017), however, the total large amount of SNF makes it difficult to be sensitive to quantities of interest in the context of either nonproliferation or safety of the repository: even the loss of one cask with a few MTU, in either case, would be significant, but this is far less

[8]Cumulative fission yield is the sum of the number of atoms per fission produced directly by the fission and those arising from decays of other fission products.

than 1% of the inventory. Effectively the remaining 99.x% of SNF blinds the neutrino detector. This situation would improve if directional neutrino detection in large detectors, hundreds or thousands of tons, became available, which potentially could be achieved by liquid argon time projection chambers, as discussed in Sec. VI.C.

Industrial-scale reprocessing results in significant quantities of liquid, highly radioactive wastes. Historically, for the nuclear weapons programs of the U.S. and the USSR, these wastes have been stored in underground tank farms and their corrosion presents a major problem due to the risk of ground water contamination (Jaraysi *et al.*, 2006; Rockhold *et al.*, 2012). Given that ^{90}Sr is extracted into the aqueous phase in the PUREX[9] process, these RW tanks also contain large quantities of ^{90}Sr and thus are the source of detectable neutrino emissions. Brdar, Huber, and Kopp (2017) presented a study of a tank farm based on an existing site (Jaraysi *et al.*, 2006) showing that an 80-year-ton exposure can measure the ^{90}Sr content of a given tank at the 20% level. Equivalently, for a known quantity of reprocessed fuel this allows an age determination in the range of 44–54 years for a true age of 50 years. This capability could be useful in clarifying the history of a plutonium-based weapons program.

In the previous example, the location of the RW was known but the quantity was not. The logical extension is the case where also the location is not known precisely. This situation could arise naturally when undeclared reprocessing is suspected and the goal is to obtain a rough estimate of the possibly extracted amount of plutonium. Such a scenario was encountered by the IAEA in 1992 in dealing with North Korea: isotopic analysis of samples taken during inspection indicated three reprocessing campaigns, whereas the initial declaration stated a single reprocessing campaign. The use of a neutrino detector specifically for this case has been the subject of a detailed study (Christensen, Huber, and Jaffke, 2015): a complete reactor core of the 5 MW_e reactor corresponds to about 8 kg of plutonium if fully reprocessed. The resulting RW can be detected at a standoff of 25 m with an exposure as little as 1–2 ton years and at a standoff of 100 m with an exposure in the 50–200 ton year range. The large increase in required exposure is due to the background from the operating reactor nearby; otherwise, required exposure simply would increase as the square of the standoff.

VIII. APPLICATIONS TO NUCLEAR EXPLOSIONS: FISSION CONFIRMATION AND YIELD ESTIMATION

A. Existing approaches

The CTBT verification regime relies in part on the International Monitoring System (IMS), a global network of facilities to detect nuclear explosions. Seismic (Kvaerna and Ringdal, 2013), hydroacoustic (Lawrence, 1999), infrasound (Green and Bowers, 2010), and radio-nuclide verification (Schoeppner, 2017) technologies comprise the IMS and are distributed across 337 stations and laboratories to monitor for nuclear explosions conducted on Earth (CTBTO, 2018). Currently, the most sensitive means for detecting underground nuclear explosions are seismic, which can detect and identify explosions down to or below a yield of about 1 kt worldwide. At low yields, if radioactive gases do not leak out in detectable quantities, it is theoretically possible that an explosion could be claimed to be conventional (although mining explosions are typically ripple-fired blasts, which are seismically distinguishable from a nuclear explosion). A nuclear explosion under the ocean would be detectable via hydroacoustic waves and in the atmosphere by the characteristic double pulse of light and radioactive fallout. In space, detection satellites monitor for a pulse of x rays (National Research Council, 2012).

B. Neutrino-based approaches

For a WATCHMAN-sized Gd-doped water detector, 10^3 m^3 fiducial volume, detection of antineutrinos in coincidence with seismic events could in theory provide unambiguous signatures of a kiloton fission explosion out to a few km and a 250 kt explosion out to a few tens of km. The largest proposed detector, with a fiducial volume of ∼200 000 m^3 could detect a 1 kt fission explosion at a distance of about 20 km (Carr, Dalnoki-Veress, and Bernstein, 2018). With fiducial volumes on the order of 10^8 m^3 detectors of this type would be able to detect 1 kt fission explosions at a distance of 1000 km or a 100 kt fission explosion at a distance of 10 000 km, providing global coverage.

IX. SUMMARY AND OUTLOOK

The pursuit of practical roles for neutrinos, especially in nuclear security, goes back at least 40 years. In those four decades, our understanding of fundamental neutrino properties has improved considerably, and neutrino emissions from fission sources have been more precisely characterized. Multiple detection channels have come into use, and the IBD channel has become a workhorse for fundamental science. As we have highlighted, neutrinos were first detected at a reactor producing plutonium for nuclear weapons. In this sense, the science of neutrinos and the wider uses of nuclear fission technology have long shared a link.

Any successful application of neutrinos will reconcile their unique advantage as a fission signature—the ability to pass through large amounts of matter—with the flip side of that property, the difficulty of identifying these particles in significant numbers in a realistic detector. This central constraint favors applications in which the flux of neutrinos is high. Of the three fission sources considered here, operating reactors have the highest time-averaged flux on timescales relevant for security problems, hours to months, at distances reasonable for observation, several meters to hundreds of kilometers.

For this reason, reactors are the most promising target for neutrino applications in the near term. As we have outlined, neutrinos may be useful for two different regimes of reactor monitoring. The first case is near-field monitoring, $\lesssim$1 km standoff, of known reactors. In near-field scenarios, few-ton-scale scintillator detectors with linear dimensions of several

[9]PUREX stands for Plutonium Uranium Redox Extraction and is the most common reaction used for reprocessing of SNF.

meters can detect on or off transitions, track power levels, meet IAEA standards for spotting plutonium diversion, and meaningfully track plutonium disposition. Detector technologies providing the requisite energy resolution and background rejection have been recently demonstrated. With modest further investment, these technologies could be deployed as a real-time, less invasive complement to existing reactor verification techniques.

A second and more ambitious application for reactor neutrinos is the discovery of hidden, undeclared reactors. This capacity would be most valuable when the sensitive range of the detector covers distances of several hundred kilometers or more, extending over wide territories and possibly national boundaries. That aspiration calls for detectors as large as the multimegaton scale with 100 m or larger in linear dimensions. While the engineering challenges and costs of megaton-scale detectors are formidable, systems on this scale are under active development for basic science. However, the background stemming from known civilian nuclear reactors presents a major obstacle and only event-by-event measurement of the neutrino direction can overcome this limitation. On the other hand, for the distance range from tens to hundreds of kilometers, the key enabling technologies for suitably large detectors are well developed: in the next decade, the WATCHMAN program expects to demonstrate reactor discovery capabilities in a 1 kt fiducial mass detector at a distance of 25 km (Askins *et al.*, 2015).

While the other stages in the nuclear fuel cycle offer opportunities for neutrino monitoring, they present considerably more challenging detection problems than operating reactors. The emission rates and energies of neutrinos emitted from SNF and reprocessing waste are lower than from reactors. Still, ton-scale scintillator detectors offer rare capabilities for verifying the contents of sealed spent fuel casks and identifying well-concealed reprocessing waste. The burst of neutrinos following an underground nuclear weapon test could help formally identify its fission nature when combined with seismic data. However, even megaton-scale detectors could surveil only a limited geographic region and would minimally enhance the strong forensic power of the existing explosion monitoring network.

This Colloquium focused on mature technologies, namely, detectors for IBD, which has now been observed over 5×10^6 times in basic science experiments at nuclear reactors. Technologies continuing to emerge from basic science, such as detectors for CEνNS, may eventually create new application options. CEνNS offers the possibility of detecting neutrinos from breeding reactions, which are below the IBD threshold, and may allow for smaller active detector masses. CEνNS was observed for the first time in 2017 (Akimov *et al.*, 2017) with neutrinos from a spallation neutron source, yet no confirmed detection of reactor neutrino via this reaction exists. The first definitive measurement of CEνNS from the reactor neutrino signal will likely first be accomplished with ionization-based detectors. However, such detectors suffer an impractical limit on their minimum size, essentially imposed by the relatively large amount of energy, 10–20 eV, needed to create a single ionization event. To realize practical detectors that are smaller than IBD detectors at a given standoff, very low-threshold, (e.g., phonon-sensitive) CEνNS detectors will need to be developed, then scaled to useful sizes. Directionality and spectroscopy via the CEνN channel are even more difficult to achieve. As a result, CEνNS-based approaches are unlikely to compete with IBD-based monitoring for a decade or longer. Note that in the case of IBD it took more than 60 years from the first detection to detectors which are capable of a safeguards mission.

Over several decades, physicists have conceived many ideas for using fission neutrinos in nuclear security. Some ideas remain in the realm of pen and paper, constrained by basic physical and practical considerations. For other concepts, demonstrated technology is catching up with real opportunities. The unique safeguard capabilities provided by near-field monitors, in particular, the ability to recover lost continuity of knowledge, make a first application more likely in cases where there is a lack of a well-established history of safeguards and mutual trust. This seems to favor applications within the verification provisions of bilateral or multilateral agreements between nations, instead of a regular safeguards agreement between a nation and the IAEA. In this context, also cost would be much less of a concern. For near-field reactor monitoring, in particular, technology now exists to support the first on-the-ground applications.

ACKNOWLEDGMENTS

The authors acknowledge extensive discussions with Rachel Carr and Frank von Hippel that took place during the preparation of this Colloquium, and Viascheslav Li for calculations of oscillated spectra and rates for reactors at large standoff. This document has been approved for release by Lawrence Livermore National Laboratory with tracking number LLNL-JRNL-784940. This work was performed under the auspices of the U.S. Department of Energy by Lawrence Livermore National Laboratory under Contract No. DE-AC52-07NA27344. This material is based upon work supported in part by the Department of Energy National Nuclear Security Administration Office of Defense Nuclear Nonproliferation R&D at Lawrence Livermore National Laboratory and through the Nuclear Science and Security Consortium under Award No. DE-NA0003180, the Consortium for Verification Technology under Award No. DE-NA0002534, the Consortium for Nonproliferation Enabling Capabilities via Award No. DE-NA0002576, and the Consortium for Monitoring, Technology and Verification under Award No. DE-NA0003920. P. H. was supported by the U.S. Department of Energy Office of Science under Award No. DE-SC0018327.

REFERENCES

Abazajian, K. N., *et al.*, 2012, "Light Sterile Neutrinos: A White Paper," arXiv:1204.5379.

Abe, Y., *et al.* (Double Chooz Collaboration), 2012, "Indication of reactor $\bar{\nu}_e$ disappearance in the double chooz experiment," Phys. Rev. Lett. **108**, 131801.

Abreu, Y., *et al.* (SoLid Collaboration), 2018a, "Optimisation of the scintillation light collection and uniformity for the SoLid experiment," J. Instrum. **13**, P09005–P09005.

Abreu, Y., *et al.* (SoLid Collaboration), 2018b, "Performance of a full scale prototype detector at the BR2 reactor for the SoLid experiment," J. Instrum. **13**, P05005–P05005.

Adey, D., *et al.* (Daya Bay Collaboration), 2019, "Extraction of the ^{235}U and ^{239}Pu Antineutrino Spectra at Daya Bay," Phys. Rev. Lett. **123**, 111801.

Ahn, J. K., *et al.* (RENO Collaboration), 2012, "Observation of Reactor Electron Antineutrino Disappearance in the RENO Experiment," Phys. Rev. Lett. **108**, 191802.

Akimov, D., *et al.* (COHERENT Collaboration), 2017, "Observation of Coherent Elastic Neutrino-Nucleus Scattering," Science **357**, 1123–1126.

Alekseev, I., *et al.* (DANSS Collaboration), 2018, "Search for sterile neutrinos at the DANSS experiment," Phys. Lett. B **787**, 56–63.

Alekseev, I. G., *et al.*, 2019, "Industrial Reactor Power Monitoring Using Antineutrino Counts in the DANSS Detector," Phys. At. Nucl. **82**, 415–424.

Almazán, H., *et al.* (STEREO Collaboration), 2018, "Sterile Neutrino Constraints from the STEREO Experiment with 66 Days of Reactor-On Data," Phys. Rev. Lett. **121**, 161801.

An, F., *et al.* (JUNO Collaboration), 2016, "Neutrino physics with JUNO," J. Phys. G **43**, 030401.

An, F. P., *et al.* (Daya Bay Collaboration), 2012, "Observation of Electron-Antineutrino Disappearance at Daya Bay," Phys. Rev. Lett. **108**, 171803.

An, F. P., *et al.* (Daya Bay Collaboration), 2016, "Measurement of the Reactor Antineutrino Flux and Spectrum at Daya Bay," Phys. Rev. Lett. **116**, 061801; **118**, 099902(E) (2017).

Apollonio, M., *et al.* (CHOOZ Collaboration), 1999, "Limits on neutrino oscillations from the CHOOZ experiment," Phys. Lett. B **466**, 415–430.

Ashenfelter, J., *et al.* (PROSPECT Collaboration), 2016, "The PROSPECT physics program," J. Phys. G **43**, 113001.

Ashenfelter, J., *et al.* (PROSPECT Collaboration), 2018a, "First search for short-baseline neutrino oscillations at HFIR with PROSPECT," Phys. Rev. Lett. **121**, 251802.

Ashenfelter, J., *et al.* (PROSPECT Collaboration), 2018b, "Performance of a segmented ^{6}Li-loaded liquid scintillator detector for the PROSPECT experiment," J. Instrum. **13**, P06023–P06023.

Ashenfelter, J., *et al.* (PROSPECT Collaboration), 2019, "Measurement of the Antineutrino Spectrum from ^{235}U Fission at HFIR with PROSPECT," Phys. Rev. Lett. **122**, 251801.

Askins, M., *et al.* (WATCHMAN Collaboration), 2015, "The Physics and Nuclear Nonproliferation Goals of WATCHMAN: A WAter CHerenkov Monitor for ANtineutrinos," arXiv:1502.01132.

Barna, Andrew, and Steve Dye, 2015, "Global Antineutrino Modeling: A Web Application," arXiv:1510.05633.

Beacom, John F., 2010, "The diffuse supernova neutrino background," Annu. Rev. Nucl. Part. Sci. **60**, 439–462.

Beacom, John F., and Mark R. Vagins, 2004, "GADZOOKS! Antineutrino spectroscopy with large water Cherenkov detectors," Phys. Rev. Lett. **93**, 171101.

Bellini, G., A. Ianni, L. Ludhova, F. Mantovani, and W. F. McDonough, 2013, "Geo-neutrinos," Prog. Part. Nucl. Phys. **73**, 1–34.

Bernstein, A., N. S. Bowden, A. Misner, and T. Palmer, 2008, "Monitoring the thermal power of nuclear reactors with a prototype cubic meter antineutrino detector," J. Appl. Phys. **103**, 074905.

Bernstein, Adam, Nathaniel S. Bowden, and Anna S. Erickson, 2018, "Reactors as a source of antineutrinos: the effect of fuel loading and burnup for mixed oxide fuels," Phys. Rev. Applied **9**, 014003.

Bernstein, Adam, Todd West, and Vipin Gupta, 2001, "An assessment of antineutrino detection as a tool for monitoring nuclear explosions," Science & Global Security **9**, 235–255.

Bethe, H., and R. Peierls, 1934, "The 'neutrino'," Nature (London) **133**, 532.

Boehm, F., *et al.*, 2001, "Final results from the Palo Verde neutrino oscillation experiment," Phys. Rev. D **64**, 112001.

Boireau, G., *et al.* (Nucifer Collaboration), 2016, "Online Monitoring of the Osiris Reactor with the Nucifer Neutrino Detector," Phys. Rev. D **93**, 112006.

Borovoi, A. A., and L. A. Mikaelyan, 1978, "Possibilities of the practical use of neutrinos," Sov. At. Energy **44**, 589–592.

Bowden, N. S., 2008, "Reactor monitoring and safeguards using antineutrino detectors," J. Phys. Conf. Ser. **136**, 022008.

Bowden, N. S., A. Bernstein, S. Dazeley, R. Svoboda, A. Misner, and T. Palmer, 2009, "Observation of the Isotopic Evolution of PWR Fuel Using an Antineutrino Detector," J. Appl. Phys. **105**, 064902.

Bowden, N. S., M. Sweany, and S. Dazeley, 2012, "A note on neutron capture correlation signals, backgrounds, and efficiencies," Nucl. Instrum. Methods Phys. Res., Sect. A **693**, 209–214.

Bowden, N. S., *et al.*, 2007, "Experimental results from an antineutrino detector for cooperative monitoring of nuclear reactors," Nucl. Instrum. Methods Phys. Res., Sect. A **572**, 985–998.

Brdar, Vedran, Patrick Huber, and Joachim Kopp, 2017, "Antineutrino monitoring of spent nuclear fuel," Phys. Rev. Applied **8**, 054050.

Brooks, F. D., 1959, "A scintillation counter with neutron and gamma-ray discriminators," Nucl. Instrum. Methods **4**, 151–163.

Carr, Rachel, Jonathon Coleman, Mikhail Danilov, Giorgio Gratta, Karsten Heeger, Patrick Huber, YuenKeung Hor, Takeo Kawasaki, Soo-Bong Kim, and Yeongduk Kim, 2019, "Neutrino-based tools for nuclear verification and diplomacy in North Korea," Science & Global Security **27**, 15–28.

Carr, Rachel, Ferenc Dalnoki-Veress, and Adam Bernstein, 2018, "Sensitivity of seismically cued antineutrino detectors to nuclear explosions," Phys. Rev. Applied **10**, 024014.

Carroll, J., J. Coleman, G. Davies, M. Lockwood, C. Metelko, R. Mills, M. Murdoch, A. Roberts, Y. Schnellbach, and C. Touramanis, 2018, "Monitoring Reactor Anti-Neutrinos Using a Plastic Scintillator Detector in a Mobile Laboratory," arXiv:1811.01006.

Castelvecchi, Davide, 2019, "Gigantic Japanese detector prepares to catch neutrinos from supernovae," Nature (London) **566**, 438–439.

Cavaignac, J. F., A. Hoummada, D. H. Koang, B. Vignon, Y. Declais, H. de Kerret, H. Pessard, and J. M. Thenard, 1984, "Indication for Neutrino Oscillation From a High Statistics Experiment at the Bugey Reactor," Phys. Lett. **148B**, 387–394.

Chen, J. D., A. F. Gerwing, and P. D. Lewis, 2001, "Long-cooled spent fuel verification using a digital Cerenkov viewing device," Technical Report No. IAEA-SM–367 (IAEA).

Choi, J. H., *et al.* (RENO Collaboration), 2016, "Observation of Energy and Baseline Dependent Reactor Antineutrino Disappearance in the RENO Experiment," Phys. Rev. Lett. **116**, 211801.

Christensen, Eric, Patrick Huber, and Patrick Jaffke, 2015, "Antineutrino Reactor Safeguards: A Case Study of the DPRK 1994 Nuclear Crisis," Science & Global Security **23**, 20–47.

Christensen, Eric, Patrick Huber, Patrick Jaffke, and Thomas E. Shea, 2014, "Antineutrino monitoring for heavy water reactors," Phys. Rev. Lett. **113**, 042503.

Classen, T., A. Bernstein, N. S. Bowden, B. Cabrera-Palmer, A. Ho, G. Jonkmans, L. Kogler, D. Reyna, and B. Sur, 2015, "Development of an advanced antineutrino detector for reactor monitoring," Nucl. Instrum. Methods Phys. Res., Sect. A **771**, 139–146.

Cogswell, Bernadette K., and Patrick Huber, 2016, "Detection of breeding blankets using antineutrinos," Science & Global Security **24**, 114–130.

Cowan, C. L., F. Reines, F. B. Harrison, H. W. Kruse, and A. D. McGuire, 1956, "Detection of the free neutrino: a confirmation," Science **124**, 103–104.

CTBTO, 2018a, "CTBTO preparatory commission—map of facilities," Accessed: 2018-05-15.

Davis, Jay C., and David A. Kay, 1992, "Iraq's secret nuclear weapons program," Phys. Today **45**, No. 7, 21–27.

Declais, Y., *et al.*, 1995, "Search for neutrino oscillations at 15-meters, 40-meters, and 95-meters from a nuclear power reactor at Bugey," Nucl. Phys. **B434**, 503–534.

Dentler, Mona, Álvaro Hernández-Cabezudo, Joachim Kopp, Pedro A. N. Machado, Michele Maltoni, Ivan Martinez-Soler, and Thomas Schwetz, **2018**, "Updated Global Analysis of Neutrino Oscillations in the Presence of eV-Scale Sterile Neutrinos," J. High Energy Phys. 08, 010.

Dye, Steve, 2017, "Evaluating Reactor Antineutrino Signals for WATCHMAN," in 12th Workshop on Applied Antineutrino Physics (AAP 2016) Liverpool, UK, arXiv:1702.06117.

Eguchi, K., *et al.* (KamLAND Collaboration), 2003, "First results from KamLAND: Evidence for reactor anti-neutrino disappearance," Phys. Rev. Lett. **90**, 021802.

Findlay, Trevor, 2007, "Looking Back: The Additional Protocol," Arms Control Today, https://www.armscontrol.org/act/2007_11/Lookingback.

Freedman, Daniel Z., 1974, "Coherent effects of a weak neutral current," Phys. Rev. D **9**, 1389–1392.

U.S. Government Accountability Office, 2014, "Spent nuclear fuel management," Technical Report No. GAO-15-141 (U.S. Government Accounting Office).

Garrett, A. J., M. Casterline, and C. Salvaggio, 2010, "Thermodynamics of Partially Frozen Cooling Lakes," Proc. SPIE Int. Soc. Opt. Eng., Thermosense XXXII **7661**, 766105.

Green, D. N., and D. Bowers, 2010, "Estimating the detection capability of the International Monitoring System infrasound network," J. Geophys. Res.: Atmos. **115**, 1–18.

Greenwood, Z. D., *et al.*, 1996, "Results of a two position reactor neutrino oscillation experiment," Phys. Rev. D **53**, 6054–6064.

Hafemeister, David W., 1989, "Infrared monitoring of nuclear power in space," Science & Global Security **1**, 109–128.

Haghighat, Alireza, Patrick Huber, Shengchao Li, Jonathan M. Link, Camillo Mariani, Jaewon Park, and Tulasi Subedi, 2018, "Observation of Reactor Antineutrinos with a Rapidly-Deployable Surface-Level Detector," arXiv:1812.02163.

Hayes, Anna C., and Petr Vogel, 2016, "Reactor neutrino spectra," Annu. Rev. Nucl. Part. Sci. **66**, 219–244.

Hecker, Siefried S., Robert L. Carlin, and Elliot A. Serbin, 2018, "A technical and political history of North Korea's nuclear program over the past 26 years," Center for International Security and Cooperation, Stanford University, https://cisac.fsi.stanford.edu/content/cisac-north-korea.

Hellfeld, D., A. Bernstein, S. Dazeley, and C. Marianno, 2017, "Reconstructing the direction of reactor antineutrinos via electron scattering in gd-doped water cherenkov detectors," Nucl. Instrum. Methods Phys. Res., Sect. A **841**, 130–138.

Huber, Patrick, 2011, "Determination of antineutrino spectra from nuclear reactors," Phys. Rev. C **84**, 024617.

Huber, Patrick, and Patrick Jaffke, 2016, "Neutron capture and the antineutrino yield from nuclear reactors," Phys. Rev. Lett. **116**, 122503.

IAEA, 1998, "Model protocol additional to the agreement(s) between state(s) and the international atomic energy agency for the application of safeguards," https://www.iaea.org/sites/default/files/infcirc540c.pdf.

IAEA, 2011, *Safeguards Techniques and Equipment*: International Nuclear Verification Series No. 1 (Rev. 2) (International Atomic Energy Agency, Vienna).

Jaffke, Patrick, and Patrick Huber, 2017, "Determining reactor fuel type from continuous antineutrino monitoring," Phys. Rev. Applied **8**, 034005.

Jaraysi, M. N., J. G. Kristofzski, M. P. Connelly, M. I. Wood, A. J. Knepp, and R. A. Quintero, 2006, "Initial Single-Shell Tank System Performance Assessment for the Hanford Site," Technical Report No. DOE/ORP-2005-01, Rev 0 (United States Nuclear Regulatory Commission, Department of Energy).

Jocher, Glenn R., Daniel A. Bondy, Brian M. Dobbs, Stephen T. Dye, James A. Georges, John G. Learned, Christopher L. Mulliss, and Shawn Usman, 2013, "Theoretical antineutrino detection, direction and ranging at long distances," Phys. Rep. **527**, 131–204.

Johnston, Roger G., Anthony R. E. Garcia, and Adam N. Pacheco, 1983, Efficacy of Tamper-Indicating Devices, Technical Report No. LAUR-02-0492 (Los Alamos National Laboratory).

Kajita, Takaaki, 2016, "Nobel Lecture: Discovery of atmospheric neutrino oscillations," Rev. Mod. Phys. **88**, 030501.

Kiff, Scott D., Nathaniel Bowden, Jim Lund, and David Reyna, 2011, "Neutron detection and identification using zns:ag/^{6}lif in segmented antineutrino detectors," Nucl. Instrum. Methods Phys. Res., Sect. A **652**, 412–416.

Klimov, Yu A., V. I. Kopeikin, L. A. Mikaélyan, K. V. Ozerov, and V. V. Sinev, 1994, "Neutrino method remote measurement of reactor power and power output," At. Energ. **76**, 123–127.

Ko, Y. J., *et al.* (NEOS Collaboration), 2017, "Sterile Neutrino Search at the NEOS Experiment," Phys. Rev. Lett. **118**, 121802.

Krauss, Lawrence M., Sheldon L. Glashow, and David N. Schramm, 1984, "Anti-neutrinos Astronomy and Geophysics," Nature (London) **310**, 191–198.

Kristensen, Hans M., and Robert S. Norris, 2013, "Global nuclear weapons inventories, 1945–2013," Bull. At. Sci. **69**, 75–81.

Kristensen, Hans M., and Robert S. Norris, 2017, "Worldwide deployments of nuclear weapons, 2017," Bull. At. Sci. **73**, 289–297.

Kudryavtsev, V. A., 2009, "Muon simulation codes music and musun for underground physics," Comput. Phys. Commun. **180**, 339–346.

Kuroda, Y., S. Oguri, Y. Kato, R. Nakata, Y. Inoue, C. Ito, and M. Minowa, 2012, "A mobile antineutrino detector with plastic scintillators," Nucl. Instrum. Methods Phys. Res., Sect. A **690**, 41–47.

Kuvshinnikov, A. A., *et al.*, 1991, "Precise measurement of the cross section for the inverse beta decay reaction at a reactor of the rovno nuclear power plant," JETP Lett. **54**, 253, http://www.jetpletters.ac.ru/ps/1248/article_18875.pdf.

Kvaerna, Tormod, and Frode Ringdal, 2013, "Detection capability of the seismic network of the International Monitoring System for the comprehensive Nuclear-Test-Ban Treaty," Bull. Seismol. Soc. Am. **103**, 759–772.

Kwon, H., F. Boehm, A. A. Hahn, H. E. Henrikson, J. L. Vuilleumier, J. F. Cavaignac, D. H. Koang, B. Vignon, F. Von Feilitzsch, and R. L. Mossbauer, 1981, "Search for Neutrino Oscillations at a Fission Reactor," Phys. Rev. D **24**, 1097–1111.

Lane, C., *et al.* (NuLat Collaboration), 2015, "A new type of Neutrino Detector for Sterile Neutrino Search at Nuclear Reactors and Nuclear Nonproliferation Applications," arXiv:1501.06935.

Langanke, K., P. Vogel, and E. Kolbe, 1996, "Signal for supernova ν_μ and ν_τ neutrinos in water Čerenkov detectors," Phys. Rev. Lett. **76**, 2629–2632.

Lasserre, Thierry, Maximilien Fechner, Guillaume Mention, Romain Reboulleau, Michel Cribier, Alain Letourneau, and David Lhuillier,

2010, "SNIF: A Futuristic Neutrino Probe for Undeclared Nuclear Fission Reactors," arXiv:1011.3850.

Lawrence, Martin W., 1999, "Overview of the hydroacoustic monitoring system for the Comprehensive Nuclear-Test-Ban Treaty," J. Acoust. Soc. Am. **105**, 1037.

Lee, Si Young, and Alfred J. Garrett, 2015, "Thermal Hydraulic Analysis for Cooling Tower Performance," in *16th International Topical Meeting on Nuclear Reactor Thermal Hydraulics* (American Nuclear Society), pp. 1074–1087, http://glc.ans.org/nureth-16/data/papers/13054.pdf#page=1.

Lilienthal, David E., Chester I. Barnard, Charles A. Thomas, J. R. Oppenheimer, and Harry A. Winne, 1946, Report on the International Control of Atomic Energy, Department of State, Publication 2498 (U.S. Government Printing Office).

Littlejohn, B. R., A. Conant, D. A. Dwyer, A. Erickson, I. Gustafson, and K. Hermanek, 2018, "Impact of Fission Neutron Energies on Reactor Antineutrino Spectra," Phys. Rev. D **97**, 073007.

McDonald, Arthur B., 2016, "Nobel Lecture: The sudbury neutrino observatory: Observation of flavor change for solar neutrinos," Rev. Mod. Phys. **88**, 030502.

Mei, D.-M., and A. Hime, 2006, "Muon-induced background study for underground laboratories," Phys. Rev. D **73**, 053004.

Mention, G., M. Fechner, Th. Lasserre, Th. A. Mueller, D. Lhuillier, M. Cribier, and A. Letourneau, 2011, "Reactor antineutrino anomaly," Phys. Rev. D **83**, 073006.

Mikaelyan, L. A., 1978, "Neutrino laboratory in the atomic plant," in *Neutrino 77, Proceedings of the International Conference on Neutrino Physics and Neutrino Astrophysics* (Nauka), Vol. 2, p. 383.

Mueller, Th. A., *et al.*, 2011, "Improved predictions of reactor antineutrino spectra," Phys. Rev. C **83**, 054615.

Mulmule, D., S. P. Behera, P. K. Netrakanti, D. K. Mishra, V. K. S. Kashyap, V. Jha, L. M. Pant, B. K. Nayak, and A. Saxena, 2018, "A plastic scintillator array for reactor based anti-neutrino studies," Nucl. Instrum. Methods Phys. Res., Sect. A **911**, 104–114.

NAS, 2016, *Lessons Learned from the Fukushima Nuclear Accident for Improving Safety and Security of U.S. Nuclear Plants: Phase 2* (The National Academies Press, Washington, DC).

National Research Council, 2012, *The Comprehensive Nuclear Test Ban Treaty: Technical Issues for the United States* (The National Academies Press, Washington, DC).

Nuclear Energy Agency, 2017, "Joint evaluated fission and fusion file (jeff) 3.3," https://www.oecd-nea.org/dbdata/jeff/jeff33/.

Nuclear Threat Initiative, 2018, "Proposed Fissile Material Cut-off Treaty," https://www.nti.org/learn/treaties-and-regimes/proposed-fissile-material-cut-off-treaty/.

NYT, 2018, "How to spot a nuclear bomb program? look for ghostly particles."

Oguri, S., Y. Kuroda, Y. Kato, R. Nakata, Y. Inoue, C. Ito, and M. Minowa, 2014, "Reactor antineutrino monitoring with a plastic scintillator array as a new safeguards method," Nucl. Instrum. Methods Phys. Res., Sect. A **757**, 33–39.

Pushkarjov, V., and E. Tkharev, 1986, "International safeguards aspects of spent-fuel storage," IAEA Bulletin, pp. 53–57.

Reines, F., H. W. Sobel, and E. Pasierb, 1980, "Evidence for Neutrino Instability," Phys. Rev. Lett. **45**, 1307.

Reines, Fred, 1995, "Nobel Lecture: The neutrino: From poltergeist to particle," https://www.nobelprize.org/prizes/physics/1995/reines/lecture/.

Renshaw, A., *et al.* (The Super-Kamiokande Collaboration), 2014, "First indication of terrestrial matter effects on solar neutrino oscillation," Phys. Rev. Lett. **112**, 091805.

Reyna, D., N. S. Bowden, A. Bernstein, S. Dazeley, G. Keefer, B. Cabrera-Palmer, T. Classen, S. Kiff, L. Kogler, and A. Erickson, 2012, "A compact and portable antineutrino detector for reactor monitoring," in *53th Annual Meeting of the Institute of Nuclear Materials Management* (Institute for Nuclear Materials Management), p. 3300.

Richelson, J. T., 2007, *Spying on the Bomb: American Nuclear Intelligence from Nazi Germany to Iran and North Korea* (W. W. Norton & Company, New York).

Riley, S. P., Z. D. Greenwood, W. R. Kropp, L. R. Price, F. Reines, H. W. Sobel, Y. Declais, A. Etenko, and M. Skorokhvatov, 1999, "Neutrino induced deuteron disintegration experiment," Phys. Rev. C **59**, 1780–1789.

Rockhold, M. L., D. H. Bacon, V. L. Freedman, M. J. Lindber, and R. E. Clayton, 2012, "Numerical Modeling of ^{90}Sr and ^{137}Cs Transport from a Spill in the B-Cell of the 324 Building, Hanford Site 300 Area," Technical Report No. PNNL-21214 (Pacific Northwest National Laboratory).

Saey, P. R. J., 2007, "Ultra-low-level measurements of argon, krypton and radioxenon for treaty verification," ESARDA Bulletin **36**, 42–56.

Safdi, Benjamin R., and Burkhant Suerfu, 2015, "Directional antineutrino detection," Phys. Rev. Lett. **114**, 071802.

Sargent, B. W., 1933, "The maximum energy of the β-Rays from uranium X and other bodies," Proc. R. Soc. A **139**, 659.

Schoeppner, Michael, 2017, "Performance Assessment of the CTBTO Noble Gas Network to Detect Nuclear Explosions," Pure Appl. Geophys. **174**, 2161–2171.

Serebrov, A. P., *et al.* (NEUTRINO-4 Collaboration), 2019, "First Observation of the Oscillation Effect in the Neutrino-4 Experiment on the Search for the Sterile Neutrino," Pis'ma Zh. Eksp. Teor. Fiz. **109**, 209–218 [JETP Lett. **109**, 213 (2019)].

Stubbs, C. W., and S. D. Drell, 2013, "Public domain treaty compliance verification in the digital age," IEEE Technology and Society Magazine **32**, 57–64.

Stumpf, Waldo, 1996, "South Africa's nuclear weapons program: From deterrence to dismantlement," Arms Control Today **25**, 3–8, www.jstor.org/stable/23625371.

United Nations Office for Disarmament Affairs, 1968, "Treaty on the Non-Proliferation of Nuclear Weapons," https://www.un.org/disarmament/wmd/nuclear/npt.

United Nations Office for Disarmament Affairs, 1996, "Comprehensive Nuclear-Test-Ban Treaty," https://www.un.org/disarmament/wmd/nuclear/ctbt/.

Usman, Shawn M., Glenn R. Jocher, Stephen T. Dye, William F. McDonough, and John G. Learned, 2015, "AGM2015: Antineutrino Global Map 2015," Sci. Rep. **5**, 13945.

van Eijk, C. W. E., A. Bessière, and P. Dorenbos, 2004, "Inorganic thermal-neutron scintillators," Nucl. Instrum. Methods Phys. Res., Sect. A **529**, 260–267.

Vidyakin, G. S., *et al.*, 1994, "Limitations on the characteristics of neutrino oscillations," JETP Lett. **59**, 390, http://www.jetpletters.ac.ru/ps/1307/article_19752.pdf.

Vogel, P., and J. F. Beacom, 1999, "Angular distribution of neutron inverse beta decay, $\bar{\nu}_e + \vec{p} e^+ + n$," Phys. Rev. D **60**, 053003.

Wahl, C. G., W. Kaye, W. Wang, F. Zhang, J. Jaworski, Y. A. Boucher, A. King, and Z. He, 2014, "Polaris-h measurements and performance," in *2014 IEEE Nuclear Science Symposium and Medical Imaging Conference (NSS/MIC)* (IEEE, New York), pp. 1–4.

Willig, Thomas Mo, Cecilia Futsaether, and Halvor Kippe, 2012, "Converting the iranian heavy water reactor ir-40 to a more proliferation-resistant reactor," Sci. Global Secur. **20**, 97–116.

World Nuclear Association, 2019, "Number of nuclear reactors operable and under construction," http://www.world-nuclear.org/nuclear-basics/global-number-of-nuclear-reactors.aspx.

Xu, Chenyuan, 2016, "Current status of SK-Gd project and EGADS," J. Phys. Conf. Ser. **718**, 062070.

Zacek, G., *et al.*, 1986, "Neutrino Oscillation Experiments at the Gosgen Nuclear Power Reactor," Phys. Rev. D **34**, 2621–2636.

Zendel, Manfred, D. L. Donohue, Erwin Kuhn, Stein Deron, and Tamas Biro, 2011, "Nuclear safeguards verification measurement techniques," *Handbook of Nuclear Chemistry* (Springer, New York).